



HAL
open science

Constraints on dark matter particles from theory, galaxy observations, and N-body simulations

Daniel Boyanovsky, Hector J. de Vega, Norma G. Sánchez

► To cite this version:

Daniel Boyanovsky, Hector J. de Vega, Norma G. Sánchez. Constraints on dark matter particles from theory, galaxy observations, and N-body simulations. *Physical Review D*, 2008, 77, pp.43518. 10.1103/PhysRevD.77.043518 . hal-03742718

HAL Id: hal-03742718

<https://hal.science/hal-03742718>

Submitted on 9 Sep 2022

HAL is a multi-disciplinary open access archive for the deposit and dissemination of scientific research documents, whether they are published or not. The documents may come from teaching and research institutions in France or abroad, or from public or private research centers.

L'archive ouverte pluridisciplinaire **HAL**, est destinée au dépôt et à la diffusion de documents scientifiques de niveau recherche, publiés ou non, émanant des établissements d'enseignement et de recherche français ou étrangers, des laboratoires publics ou privés.

Constraints on dark matter particles from theory, galaxy observations, and N -body simulations

D. Boyanovsky,^{1,2,3,*} H. J. de Vega,^{3,2,1,†} and N. G. Sanchez^{2,‡}

¹*Department of Physics and Astronomy, University of Pittsburgh, Pittsburgh, Pennsylvania 15260, USA*

²*Observatoire de Paris, LERMA, Laboratoire Associé au CNRS UMR 8112, 61, Avenue de l'Observatoire, 75014 Paris, France*

³*LPTHE, Université Pierre et Marie Curie (Paris VI) et Denis Diderot (Paris VII),*

Laboratoire Associé au CNRS UMR 7589, Tour 24, 5ème. étage, 4, Place Jussieu, 75252 Paris, Cedex 05, France

(Received 26 October 2007; published 19 February 2008)

Mass bounds on dark matter (DM) candidates are obtained for particles that decouple in or out of equilibrium while ultrarelativistic with *arbitrary* isotropic and homogeneous distribution functions. A coarse grained Liouville invariant primordial phase-space density \mathcal{D} is introduced which depends solely on the distribution function at decoupling. The density \mathcal{D} is explicitly computed and combined with recent photometric and kinematic data on dwarf spheroidal satellite galaxies in the Milky Way (dShps) and the observed DM density today yielding upper and lower bounds on the mass, primordial phase-space densities, and velocity dispersion of the DM candidates. Combining these constraints with recent results from N -body simulations yields estimates for the mass of the DM particles in the range of a few keV. We establish in this way a direct connection between the microphysics of decoupling *in or out* of equilibrium and the constraints that the particles must fulfill to be suitable DM candidates. If chemical freeze-out occurs before thermal decoupling, light bosonic particles can Bose condense. We study such Bose-Einstein condensate (BEC) as a dark matter candidate. It is shown that, depending on the relation between the critical (T_c) and decoupling (T_d) temperatures, a BEC light relic could act as cold DM but the decoupling scale must be *higher* than the electroweak scale. The condensate hastens the onset of the nonrelativistic regime and tightens the upper bound on the particle's mass. A nonequilibrium scenario which describes particle production and partial thermalization, sterile neutrinos produced out of equilibrium, and other DM models is analyzed in detail and the respective bounds on mass, primordial phase-space density, and velocity dispersion are obtained. Thermal relics with $m \sim$ few keV that decouple when ultrarelativistic and sterile neutrinos produced resonantly or nonresonantly lead to a primordial phase-space density compatible with *cored* dShps and disfavor cusped satellites. Light Bose-condensed DM candidates yield phase-space densities consistent with *cores* and if $T_c \gg T_d$ also with cusps. Phase-space density bounds on particles that decoupled nonrelativistically combined with recent results from N -body simulations suggest a potential tension for WIMPs with $m \sim 100$ GeV, $T_d \sim 10$ MeV.

DOI: [10.1103/PhysRevD.77.043518](https://doi.org/10.1103/PhysRevD.77.043518)

PACS numbers: 98.80.-k, 95.35.+d, 98.80.Cq

I. INTRODUCTION

Although the existence of dark matter (DM) was inferred several decades ago [1], its nature still remains elusive. Candidate dark matter particles are broadly characterized as cold, hot, or warm depending on their velocity dispersions. The clustering properties of collisionless DM candidates in the linear regime depend on the free-streaming length, which roughly corresponds to the Jeans length with the particle's velocity dispersion replacing the speed of sound in the gas. Cold DM (CDM) candidates feature a small free-streaming length favoring a bottom-up hierarchical approach to structure formation, smaller structures form first, and mergers lead to clustering on the larger scales.

Among the CDM candidates are weakly interacting massive particles (WIMPs) with $m \sim 10\text{--}10^2$ GeV. Hot DM (HDM) candidates feature large free-streaming lengths and favor top down structure formation, where

larger structures form first and fragment. HDM particle candidates are deemed to have masses in the few eV range, and warm DM (WDM) candidates are intermediate with a typical mass range $m \sim 1\text{--}10$ keV.

The *concordance* Λ CDM standard cosmological model emerging from cosmic microwave background (CMB), large scale structure observations, and simulations favors the hypothesis that DM is composed of primordial particles which are cold and collisionless [2]. However, recent observations hint at possible discrepancies with the predictions of the Λ CDM concordance model: the satellite and cuspy halo problems.

The satellite problem stems from the fact that CDM favors the presence of substructure: much of the CDM is not smoothly distributed but is concentrated in small lumps, in particular, in dwarf galaxies for which there is scant observational evidence so far. A low number of satellites have been observed in Milky Way sized galaxies [3–6]. This substructure is a consequence of the CDM power spectrum which favors small scales becoming non-linear first, collapsing in the bottom-up hierarchical manner, and surviving the mergers as dense clumps [4,6].

*boyan@pitt.edu

†devega@lpthe.jussieu.fr

‡Norma.Sanchez@obspm.fr

The cuspy halo problem arises from the result of large scale N -body simulations of CDM clustering which predict a monotonic increase of the density towards the center of the halos [5,7–10], for example, the universal Navarro-Frenk-White profile $\rho(r) \sim r^{-1}(r+r_0)^{-2}$ [8] which describes accurately clusters of galaxies, but indicates a divergent cusp at the center of the halo. Recent observations seem to indicate central cores in dwarf galaxies [11–14], leading to the “cusps vs cores” controversy.

A recent compilation of observations of dwarf spheroidal galaxies dSphs [14], which are considered to be prime candidates for DM substructure [15], seem to favor a core with a smoother central density and a low mean mass density $\sim 0.1M_\odot/\text{pc}^3$ rather than a cusp [14]. The data cannot yet rule out cuspy density profiles which allow a maximum density $\lesssim 60M_\odot/\text{pc}^3$ and the interpretation and analysis of the observations is not yet conclusive [11,16]. These possible discrepancies have rekindled an interest in WDM particles, which feature a velocity dispersion larger than CDM particles, and consequently larger free-streaming lengths which smooth out the inner cores and would be prime candidates to relieve the cuspy halo and satellite problems [17].

A possible WDM candidate is a sterile neutrino [18–20] with a mass in the keV range and produced via their mixing and oscillation with an active neutrino species either non-resonantly [18], or through Mikheiev-Smirnov-Wolfenstein (MSW) resonances in the medium [19]. Sterile neutrinos can decay into a photon and an active neutrino (more precisely the largest mass eigenstate decays into the lowest one and a photon) [21] yielding the possibility of direct constraints on the mass and mixing angle from the diffuse x-ray background [22].

Observations of cosmological structure formation via the Lyman- α forest provide a complementary probe of primordial density fluctuations on small scales which yield an indirect constraint on the masses of WDM candidates. While constraints from the diffuse x-ray background yield an upper bound on the mass of a putative sterile neutrino in the range 3–8 keV [22], the latest Lyman- α analysis [23] yields lower bounds in the range 10–13 keV in tension with the x-ray constraints. More recent constraints from Lyman- α yield a lower limit for the mass of a WDM candidate $m_{\text{WDM}} \gtrsim 1.2 \text{ keV}(2\sigma)$ for an early decoupled thermal relic and $m_{\text{WDM}} \gtrsim 5.6 \text{ keV}(2\sigma)$ for sterile neutrinos [24]. Strong upper limits on the mass and mixing angles of sterile neutrinos have been recently discussed [25], however, there are uncertainties as to whether WDM candidates can explain large cores in dSphs [26]. It has been recently argued [27] that if sterile neutrinos are produced nonresonantly [18] the combined x-ray and Lyman- α data suggest that these cannot be the only WDM component, with an upper limit for their fractional relic abundance $\lesssim 0.7$. Recent [28] constraints on a radiatively decaying DM particle from the EPIC spectra of

(M31) by XMM-Newton confirms this result and places a stronger lower mass limit $m < 4 \text{ keV}$.

All these results suggest that DM could be a mixture of several components with sterile neutrinos as viable candidates.

Motivation and goals.—Although the Λ CDM paradigm describes large scale structure formation remarkably well, the possible small scale discrepancies mentioned above motivate us to study new constraints that different dark matter components must fulfill to be suitable candidates. Cosmological bounds on dark matter components primarily focused on standard model neutrinos [29,30], heavy relics that decoupled in local thermodynamic equilibrium (LTE) when nonrelativistic [31–33] or thermal ultrarelativistic [34–38]. More recently, cosmological precision data were used to constrain the (HDM) abundance of low mass particles [39–42] assuming these to be thermal relics.

The main results of this article are:

- (a) We consider particles that decouple *in or out of LTE* during the radiation dominated era with an *arbitrary* (but homogeneous and isotropic) distribution function. Particles which decouple being ultrarelativistic eventually become nonrelativistic because of redshift of physical momentum. We establish a direct connection between the microphysics of decoupling in or out of LTE and the constraints that the particles must fulfill to be suitable DM candidates *in terms of the distribution functions at decoupling*.
- (b) We introduce a primordial coarse grained phase-space density

$$\mathcal{D} \equiv \frac{n(t)}{\langle \bar{p}_f^2 \rangle^{3/2}},$$

where $n(t)$ is the number of particles per unit physical volume and $\langle \bar{p}_f^2 \rangle$ is the average of the physical momentum with the distribution function of the decoupled particle. \mathcal{D} is a Liouville invariant after decoupling and only depends on the distribution functions at decoupling. In the nonrelativistic regime \mathcal{D} is simply related to the phase densities considered in Refs. [11,30,36,38] and can only decrease by collisionless phase mixing or self-gravity dynamics [43].

In the nonrelativistic regime we obtain

$$\mathcal{D} = \frac{1}{3^{3/2}m^4} \frac{\rho_{\text{DM}}}{\sigma_{\text{DM}}^3}, \quad (1.1)$$

where σ_{DM} is the primordial one-dimensional velocity dispersion and ρ_{DM} the dark matter density. Combining the result for the primordial phase-space density \mathcal{D} determined by the mass and the distribution function of the decoupled particles, with the recent compilation of photometric and kinematic data on dSphs satellites in the Milky Way [14] yields

lower bounds on the DM particle mass m whereas upper bounds on the DM mass are obtained using the value of the observed dark matter density today. Therefore the combined analysis of observational data from (d)Sphs, N -body simulations and the present DM density allows us to establish both upper and lower bounds on the mass of the DM candidates.

We thus provide a link between the microphysics of decoupling, the observational aspects of dark matter halos, and the DM mass value.

- (c) Recent N -body simulations [44] indicate that the phase-space density decreases a factor $\sim 10^2$ during gravitational clustering. This result combined with Eq. (1.1) and the observed values on dSphs satellites [14] yields

$$m_{\text{cored}} \sim \frac{2}{g^{1/4}} \text{ keV}, \quad m_{\text{cusp}} \sim \frac{8}{g^{1/4}} \text{ keV}$$

for the masses of *thermal relics* DM candidates, where “cored” and “cusp” refer to the type of profile used in the dSphs description and $1 \leq g \leq 4$ is the number of internal degrees of freedom of the DM particle. Wimps with masses ~ 100 GeV decoupling in LTE at temperatures $T_d \sim 10$ MeV lead to primordial phase-space densities many orders of magnitude larger than those observed in (d)Sphs. The results of N -body simulations, which yield relaxation by 2–3 orders of magnitude [44], suggest a potential tension for WIMPs as DM candidates. However, the N -body simulations in Ref. [44] begin with initial conditions with values of the phase-space density much lower than the primordial one. Hence, it becomes an important question whether the enormous relaxation required from the primordial values to those of observed in dSphs can be inferred from numerical studies with suitable (much larger) initial values of the phase-space density.

- (d) We study the possibility that the DM particle is a light boson that undergoes Bose-Einstein condensation (BEC) prior to decoupling while still ultrarelativistic. (This possibility was addressed in [35]). We analyze in detail the constraints on such BEC DM candidate from velocity dispersion and phase-space arguments, and contrast the BEC DM properties to those of the hot or warm thermal relics.
- (e) Nonequilibrium scenarios that describe various possible WDM candidates are studied in detail. These scenarios describe particle production [45] and incomplete thermalization [46], resonant [18] and nonresonant [19] production of sterile neutrinos, and a model recently proposed [26] to describe cores in dSphs.

Our analysis of the DM candidates is based on their masses, statistics, and properties at decoupling (being it in

LTE or not). We combine observations on dSphs [14] and N -body simulations [44], with theoretical analysis using the nonincreasing property of the phase-space density [11,30,38,43].

The results from the combined analysis of the primordial phase-space densities, the observational data on dSphs [14], and the N -body simulations in Ref. [44] are the following:

- (i) Conventional thermal relics, and sterile neutrinos produced resonantly or nonresonantly with mass in the range $m \sim \text{few keV}$ that decouple when ultrarelativistic lead to a primordial phase-space density of the same order of magnitude as in cored dSphs and disfavor cusped satellites for which the data [14] yields a much larger phase-space density.
- (ii) CDM from wimps that decouple when nonrelativistic with $m \gtrsim 100$ GeV and kinetic decoupling at $T_d \sim 10$ MeV [33] yield phase-space densities at least 18 to 15 orders of magnitude [see Eqs. (4.30), (4.31), and (4.37)] larger than the typical average in dSphs [14]. Results from N -body simulations, albeit with initial conditions with much smaller values of the phase-space density, yield a dynamical relaxation by a factor 10^2 – 10^3 [44]. If these results are confirmed by simulations with larger initial values there may be a potential tension between the primordial phase-space density for *thermal relics* in the form of WIMPs with $m \sim 100$ GeV $T_d \sim 10$ MeV and those observed in dSphs.
- (iii) Light bosonic particles decoupled while ultrarelativistic and which form a BEC lead to phase-space densities consistent with cores and also consistent with cusps if $T_c/T_d \gtrsim 10$. However, if these thermal relics satisfy the observational bounds, they must decouple when $g_d g^{-(3/4)} (T_d/T_c)^{9/8} > 130$, namely above the electroweak scale.

Section II analyzes the generic dynamics of decoupled particles for any distribution function, with or without LTE at decoupling, and for *different* species of particles. In Sec. III we consider light thermal relics which decoupled in LTE as DM components: fermions and bosons, including the possibility of a Bose-Einstein condensate. Section IV deals with coarse grained phase-space densities which are Liouville invariant and the new bounds obtained with them by using the observational dSphs data and recent results from N -body simulations, bounds from velocity dispersion, and the generalized Gunn-Tremaine bound. In Sec. V we study the case of particles that decoupled out of equilibrium and the consequences on the dark matter constraints. Section VI summarizes our conclusions.

II. PRELIMINARIES: DYNAMICS OF DECOUPLED PARTICLES

While the study of kinetics in the early Universe is available in the literature [32,47,48], in this section we

expand on the *dynamics of decoupled particles* emphasizing several aspects relevant to the analysis that follows in the next sections.

Consider a spatially flat Friedmann-Robertson-Walker (FRW) cosmology with length element

$$ds^2 = dt^2 - a^2(t)d\vec{x}^2. \quad (2.1)$$

The nonvanishing Christoffel symbols are

$$\Gamma_{ij}^0 = \dot{a}a\delta_{ij}, \quad \Gamma_{0j}^i = \Gamma_{j0}^i = \frac{\dot{a}}{a}\delta_j^i. \quad (2.2)$$

The (contravariant) four momentum is defined as $p^\mu = dx^\mu/d\lambda$ with λ an affine parameter, so that $g_{\mu\nu}p^\mu p^\nu = m^2$, where m is the mass of the particle. This leads to the dispersion relation

$$p^0(t) = \sqrt{m^2 + a^2(t)\vec{p}^2(t)}. \quad (2.3)$$

The geodesic equations are

$$\begin{aligned} \frac{dp^0}{d\lambda} &= p^0(t)\dot{p}^0 = -H(t)a^2(t)p^2(t) \Rightarrow \dot{p}^0 \\ &= -H(t)\frac{a^2(t)p^2(t)}{p^0(t)} \end{aligned} \quad (2.4)$$

$$\frac{d\vec{p}}{d\lambda} = -2H(t)p^0(t)\vec{p}(t) \Rightarrow \dot{\vec{p}} = -2H(t)\vec{p}(t),$$

where $H(t) \equiv \frac{\dot{a}}{a}$ and we used $d/d\lambda = p^0 d/dt$. The solution of Eq. (2.4) is

$$\vec{p} = \frac{\vec{p}_c}{a^2(t)}, \quad (2.5)$$

where p_c is the time independent comoving momentum. The local observables, energy, and momentum as measured by an observer at rest in the expanding cosmology are given by

$$E(t) = g_{\mu\nu}\epsilon_0^\mu p^\nu, \quad P_f^i(t) = -g_{\mu\nu}\epsilon_i^\mu p^\nu, \quad (2.6)$$

where ϵ_α^μ form a local orthonormal tetrad (vierbein)

$$g_{\mu\nu}\epsilon_\alpha^\mu\epsilon_\beta^\nu = \eta_{\alpha\beta} = \text{diag}(1, -1, -1, -1),$$

and the sign in Eq. (2.6) corresponds to a spacelike component. For the FRW metric

$$\epsilon_\alpha^\mu = \sqrt{|g^{\mu\alpha}|}, \quad (2.7)$$

and we find

$$E = p^0, \quad \vec{P}_f(t) = a(t)\vec{p}(t) = \frac{\vec{p}_c}{a(t)}. \quad (2.8)$$

\vec{P}_f is clearly the physical momentum, redshifting with the expansion. Combining the above with Eq. (2.3) yields the local dispersion relation

$$E(t) = p^0(t) = \sqrt{m^2 + \vec{P}_f^2(t)}. \quad (2.9)$$

A frozen distribution describing a particle that has been decoupled from the plasma is constant along geodesics, therefore, taking the distribution to be a function of the physical momentum \vec{P}_f and time, it obeys the Liouville equation or collisionless Boltzmann equation

$$\frac{d}{d\lambda}f[P_f; t] = 0 \Rightarrow \frac{df[P_f; t]}{dt} = 0. \quad (2.10)$$

Taking P_f as an independent variable this equation leads to the familiar form

$$\frac{\partial f[P_f; t]}{\partial t} - H(t)P_f \frac{\partial f[P_f; t]}{\partial P_f} = 0. \quad (2.11)$$

Obviously a solution of this equation is

$$f[P_f; t] \equiv f_d[a(t)P_f] = f_d[p_c], \quad (2.12)$$

where p_c is the time independent comoving momentum. The physical phase-space volume element is invariant, $d^3X_f d^3P_f = d^3x_c d^3p_c$, where f, c refer to physical and comoving volumes, respectively.

The scale factor is normalized so that

$$a(t) = \frac{1 + z_d}{1 + z(t)} \quad (2.13)$$

and $P_f(t_d) = p_c$, where t_d is the cosmic time at decoupling and z is the redshift.

If a particle of mass m has been in LTE but it decoupled from the plasma with decoupling temperature T_d , its distribution function is

$$f_d(p_c) = \frac{1}{e^{(\sqrt{m^2 + p_c^2} - \mu_d)/T_d} \pm 1}, \quad (2.14)$$

for fermions (+) or bosons (-), respectively, allowing for a chemical potential μ_d at decoupling.

In what follows we consider general distributions as in Eq. (2.12) unless specifically stated.

The kinetic energy momentum tensor associated with this frozen distribution is given by

$$T_\nu^\mu = g \int \frac{d^3P_f}{(2\pi)^3} \frac{p^\mu p_\nu}{p^0} f_d(p_c), \quad (2.15)$$

where g is the number of internal degrees of freedom, typically $1 \leq g \leq 4$. Taking the distribution function to be isotropic, it follows that

$$T_0^0 = g \int \frac{d^3P_f}{(2\pi)^3} p^0 f_d(p_c) = \rho \quad (2.16)$$

$$\begin{aligned} T_j^i &= -\frac{g}{3} \delta_j^i \int \frac{d^3P_f}{(2\pi)^3} \frac{a^2(t)p^2}{p^0} f_d(p_c) \\ &= -\frac{g}{3} \delta_j^i \int \frac{d^3P_f}{(2\pi)^3} \frac{P_f^2}{p^0} f_d(p_c) = -\delta_j^i \mathcal{P}, \end{aligned} \quad (2.17)$$

where ρ is the energy density and \mathcal{P} is the pressure. In

summary,

$$\begin{aligned}\rho &= g \int \frac{d^3 P_f}{(2\pi)^3} \sqrt{m^2 + P_f^2} f_d[a(t)P_f]; \\ \mathcal{P} &= \frac{g}{3} \int \frac{d^3 P_f}{(2\pi)^3} \frac{P_f^2}{\sqrt{m^2 + P_f^2}} f_d[a(t)P_f].\end{aligned}\quad (2.18)$$

The pressure can be written in a manner more familiar from kinetic theory as

$$\mathcal{P} = g \int \frac{d^3 P_f}{(2\pi)^3} \frac{|\vec{v}_f|^2}{3} \sqrt{m^2 + P_f^2} f_d[a(t)P_f], \quad (2.19)$$

where $\vec{v}_f = \vec{P}_f/E$ is the physical (group) velocity of the particles measured by an observer at rest in the expanding cosmology.

To confirm covariant energy conservation recall that $d^3 P_f = d^3 p_c/a^3(t)$; $P_f = p_c/a(t)$; $df_d/dt = 0$. Furthermore from Eq. (2.4) it follows that $\dot{p}^0 = -H(t)P_f^2/p^0$, leading to

$$\dot{\rho} = -3H(t)\rho - H(t)g \int \frac{d^3 P_f}{(2\pi)^3} \frac{P_f^2}{p^0} f_d(p_c), \quad (2.20)$$

the first term results from the measure and the last term from \dot{p}^0 ; from the expression of the pressure Eq. (2.17) the covariant conservation equation

$$\dot{\rho} + 3H(t)(\rho + \mathcal{P}) = 0 \quad (2.21)$$

follows. The number of particles per unit physical volume is

$$n(t) = g \int \frac{d^3 P_f}{(2\pi)^3} f_d[a(t)P_f], \quad (2.22)$$

and obeys

$$\frac{dn(t)}{dt} + 3H(t)n(t) = 0, \quad (2.23)$$

namely, the number of particles per unit *comoving* volume $n(t)a^3(t)$ is conserved.

These are generic results for the kinetic energy momentum tensor and the particle density for any distribution function that obeys the collisionless Boltzmann equation (2.10).

The entropy density for an arbitrary distribution function for particles that decoupled in or out of LTE is

$$s_d(t) = -g \int \frac{d^3 P_f}{(2\pi)^3} [f_d \ln f_d \pm (1 \mp f_d) \ln(1 \mp f_d)], \quad (2.24)$$

where the upper and lower signs refer to fermions and bosons, respectively. Since $df_d/dt = 0$ it follows that

$$\frac{ds_d(t)}{dt} + 3H(t)s_d(t) = 0, \quad (2.25)$$

therefore the entropy per *comoving* volume $s_d(t)a^3(t)$ is constant. In particular, the ratio

$$Y = \frac{n(t)}{s_d(t)} \quad (2.26)$$

is a constant for *any* distribution function that obeys the collisionless Liouville equation [32].

In the case of LTE, using the distribution equation (2.14) in the entropy density equation (2.24) yields the result

$$s_d(t) = \frac{\rho_d + P_d}{T_d a^3(t)} - \frac{\mu_d}{T_d} n(t), \quad (2.27)$$

for either statistics, where ρ_d ; P_d are evaluated at the decoupling time t_d . The entropy of the gas of decoupled particles does *not* affect the relationship between the photon temperature and the temperature of ultrarelativistic particles that decouple *later* which can be seen as follows.

Consider several species of particles, one of which decouples at an earlier time *in or out of equilibrium* with the distribution function f_d and entropy given by Eq. (2.24) while the others remain in LTE with entropy density $(2\pi^2/45)g(T)T^3$, until some of them decouple later while ultrarelativistic. Here T is the temperature at time t and $g(T)$ is the effective number of ultrarelativistic degrees of freedom. Entropy conservation leads to the relation

$$\left[\frac{2\pi^2}{45} g(T)T^3 + s_d \right] a^3(t) = \text{constant}, \quad (2.28)$$

however, because $s_d(t)a^3(t) = \text{constant}$, the usual relation $g(T)T^3 a^3(t) = \text{constant}$, relating the temperature T of a gas of ultrarelativistic decoupled particles to the photon temperature follows.

For light particles that decouple in LTE at temperature $T_d \gg m$, we can approximate

$$\frac{\sqrt{m^2 + p_c^2} - \mu_d}{T_d} \simeq \frac{p_c - \mu_d}{T_d} = \frac{P_f - \mu_d(t)}{T_d(t)}, \quad (2.29)$$

where

$$T_d(t) = \frac{T_d}{a(t)}, \quad \mu_d(t) = \frac{\mu_d}{a(t)} \quad (2.30)$$

are the decoupling temperature and chemical potential redshifted by the expansion, therefore for particles that decouple in LTE with $T_d \gg m$ we can approximate

$$f_d(P_f; t) = \frac{1}{e^{(P_f/T_d(t)) - (\mu_d(t)/T_d(t))} \pm 1} = \frac{1}{e^{(p_c - \mu_d)/T_d} \pm 1}. \quad (2.31)$$

This distribution function is the same as that of a *massless* particle in LTE which is also a solution of the Liouville equation, or collisionless Boltzmann equation.

Since the distribution function is dimensionless, without loss of generality we can always write for a particle that *decoupled in or out of LTE*

$$f_d(p_c) = f_d\left(\frac{p_c}{T_d}; \frac{m}{T_d}; \alpha_i\right), \quad (2.32)$$

where α_i are *dimensionless* constants determined by the microphysics, for example, dimensionless couplings or ratios between T_d and particle physics scales or in equilibrium μ_d/T_d etc. To simplify notation in what follows, we will not include explicitly the set of dimensionless constants m/T_d , α_i , etc., in the argument of f_d , but these are implicit in generic distribution functions. If the particle decouples when it is ultrarelativistic, $m/T_d \rightarrow 0$.

It is convenient to introduce the dimensionless ratios

$$y = \frac{p_c}{T_d} = \frac{P_f}{T_d(t)}, \quad T_d(t) = \frac{T_d}{a(t)} \quad (2.33)$$

and

$$x_d = \frac{m}{T_d}, \quad x(t) = \frac{m}{T_d(t)} = a(t)x_d. \quad (2.34)$$

For example, for a particle that decouples in equilibrium while being nonrelativistic, f_d is the Maxwell-Boltzmann distribution function [32]

$$\begin{aligned} f_d(p_c) &= \frac{2^{5/2} \pi^{7/2}}{45} g_d Y_\infty e^{-(p_c^2/2mT_d)} \\ &= \frac{2^{5/2} \pi^{7/2}}{45} g_d Y_\infty e^{-(y^2/2x_d)}, \end{aligned} \quad (2.35)$$

where g_d is the effective number of ultrarelativistic degrees of freedom at decoupling, $Y = n/s$ and Y_∞ is the solution of the Boltzmann equation, whose dependence on $x_d = m/T_d$ and the annihilation cross section is given in Chapter 5.2 in Ref. [32].

Changing the integration variable in Eqs. (2.18), (2.19), (2.20), (2.21), and (2.22) to $P_f = yT_d(t)$, we find

$$\begin{aligned} \rho &= gmT_d^3(t)I_\rho[x], \\ I_\rho[x] &= \frac{1}{2\pi^2} \int_0^\infty y^2 \sqrt{1 + \frac{y^2}{x^2}} f_d(y) dy, \\ \mathcal{P} &= g \frac{T_d^5(t)}{3m} I_{\mathcal{P}}[x], \\ I_{\mathcal{P}}[x] &= \frac{1}{2\pi^2} \int_0^\infty dy \frac{y^4 f_d(y)}{\sqrt{1 + \frac{y^2}{x^2}}} = -x^3 \frac{dI_\rho[x]}{dx}, \\ n(t) &= g \frac{T_d^3(t)}{2\pi^2} \int_0^\infty y^2 f_d(y) dy = gT_d^3(t)I_\rho[x = \infty], \end{aligned} \quad (2.36)$$

leading to the equation of state:

$$w[x] = \frac{\mathcal{P}}{\rho} = \frac{I_{\mathcal{P}}[x]}{3x^2 I_\rho[x]} = -\frac{1}{3} \frac{d \ln I_\rho[x]}{d \ln x}. \quad (2.37)$$

In the ultrarelativistic and nonrelativistic limits, $x \rightarrow 0$ and $x \rightarrow \infty$, respectively, we find

$$\begin{aligned} I_\rho[x] &\stackrel{x \rightarrow 0}{\equiv} \frac{1}{x} \int_0^\infty \frac{y^3 dy}{2\pi^2} f_d(y), \\ I_{\mathcal{P}}[x] &\stackrel{x \rightarrow 0}{\equiv} x \int_0^\infty \frac{y^3 dy}{2\pi^2} f_d(y), \\ I_\rho[x] &\stackrel{x \rightarrow \infty}{\equiv} \int_0^\infty \frac{y^2 dy}{2\pi^2} f_d(y), \\ I_{\mathcal{P}}[x] &\stackrel{x \rightarrow \infty}{\equiv} \int_0^\infty \frac{y^4 dy}{2\pi^2} f_d(y). \end{aligned} \quad (2.38)$$

In the ultrarelativistic limit the energy density and pressure become

$$\rho \stackrel{x \rightarrow 0}{\equiv} gT_d^4(t) \int_0^\infty \frac{y^3 dy}{2\pi^2} f_d(y), \quad \mathcal{P} \stackrel{x \rightarrow 0}{\equiv} \frac{\rho}{3}, \quad w[x] \stackrel{x \rightarrow 0}{\equiv} \frac{1}{3}, \quad (2.39)$$

describing radiation behavior. In the nonrelativistic limit

$$\begin{aligned} \rho &\stackrel{x \rightarrow \infty}{\equiv} mgT_d^3(t) \int_0^\infty y^2 f_d(y) \frac{dy}{2\pi^2} = mn(t), \\ \mathcal{P} &\stackrel{x \rightarrow \infty}{\equiv} \frac{gT_d^5(t)}{3m} \int_0^\infty y^4 f_d(y) \frac{dy}{2\pi^2} \rightarrow 0 \end{aligned} \quad (2.40)$$

and the equation of state becomes

$$w[x] \stackrel{x \rightarrow \infty}{\equiv} \frac{1}{3} \left[\frac{T_d(t)}{m} \right]^2 \frac{\int_0^\infty y^4 dy f_d(y)}{\int_0^\infty y^2 dy f_d(y)} \rightarrow 0, \quad (2.41)$$

corresponding to cold matter behavior. In the nonrelativistic limit, it is convenient to write

$$\begin{aligned} \rho &= mn_\gamma(t) g \left[\frac{T_d(t)}{T_\gamma(t)} \right]^3 \frac{\int_0^\infty y^2 f_{d,a}(y) dy}{4\zeta(3)} \\ &= mn_\gamma(t) \frac{g \int_0^\infty y^2 f_{d,a}(y) dy}{2g_d \zeta(3)}, \end{aligned} \quad (2.42)$$

where $\zeta(3) = 1.2020569\dots$, g_d is the number of ultrarelativistic degrees of freedom at decoupling, and $n_\gamma(t)$ is the photon number.

The average squared velocity of the particle is given in the nonrelativistic limit by

$$\begin{aligned} \langle \vec{v}^2 \rangle &= \left\langle \frac{\vec{P}_f^2}{m^2} \right\rangle = \frac{\int \frac{d^3 P_f}{(2\pi)^3} \frac{\vec{P}_f^2}{m^2} f_d[a(t)P_f]}{\int \frac{d^3 P_f}{(2\pi)^3} f_d[a(t)P_f]} \\ &= \left[\frac{T_d(t)}{m} \right]^2 \frac{\int_0^\infty y^4 f_d(y) dy}{\int_0^\infty y^2 f_d(y) dy}. \end{aligned} \quad (2.43)$$

Therefore, the equation of state in thermal equilibrium is given by

$$\mathcal{P} = \frac{1}{3} \langle \vec{v}^2 \rangle \rho \equiv \sigma^2 \rho, \quad \sigma = \sqrt{\frac{1}{3} \langle \vec{v}^2 \rangle}, \quad (2.44)$$

where σ is the *one-dimensional* velocity dispersion given at redshift z by

$$\begin{aligned}\sigma(z) &= \frac{T_d(t)}{m} \left[\frac{\int_0^\infty y^4 f_d(y) dy}{3 \int_0^\infty y^2 f_d(y) dy} \right]^{1/2} \\ &= 0.05124 \frac{1+z}{g_d^{1/3}} \left(\frac{\text{keV}}{m} \right) \left[\frac{\int_0^\infty y^4 f_d(y) dy}{\int_0^\infty y^2 f_d(y) dy} \right]^{1/2} \left(\frac{\text{km}}{\text{s}} \right)\end{aligned}\quad (2.45)$$

and we used that

$$T_d(t) = T_d(1+z) = \left(\frac{2}{g_d} \right)^{1/3} T_\gamma(1+z), \quad (2.46)$$

$T_\gamma = 0.2348 \times 10^{-3}$ eV is the photon temperature today [49].

The results above, Eqs. (2.36)–(2.45) are general for any distribution of decoupled particles *whether or not* the particles decoupled in equilibrium.

Using the relation (2.42) for a given species (a) of particles with g_a degrees of freedom, their relic abundance today is given by

$$\Omega_a h^2 = \frac{m_a}{25.67 \text{ eV}} \frac{g_a \int_0^\infty y^2 f_{d,a}(y) dy}{2g_{d,a} \zeta(3)}, \quad (2.47)$$

where we used that today $h^2 n_\gamma / \rho_c = 1/25.67$ eV [49].

If this decoupled species contributes a fraction ν_a to dark matter, with $\Omega_a = \nu_a \Omega_{\text{DM}}$ and using that $\Omega_{\text{DM}} h^2 = 0.105$ [49] for nonbaryonic dark matter, then

$$\nu_a = \frac{m_a}{2.695 \text{ eV}} \frac{g_a \int_0^\infty y^2 f_{d,a}(y) dy}{2g_{d,a} \zeta(3)}. \quad (2.48)$$

Since $0 \leq \nu_a \leq 1$ we find the constraint

$$m_a \leq 2.695 \text{ eV} \frac{2g_{d,a} \zeta(3)}{g_a \int_0^\infty y^2 f_{d,a}(y) dy}, \quad (2.49)$$

where in general f_d depends on the mass of the particle as in Eq. (2.32). For a particle that decouples while nonrelativistic with the distribution function Eq. (2.35) this is recognized as the generalization of the Lee-Weinberg *lower bound* [31,32], whereas if the particle decouples in or out of LTE when it is ultrarelativistic, in which case $f_{d,a}(y)$ does not depend on the mass, Eq. (2.49) provides an *upper bound* which is a generalization of the Cowsik-McClelland [32,50] bound.

The constraint equation (2.49) suggests *two* ways to allow for more massive particles: by increasing g_d , namely, the particle decouples earlier, at higher temperatures when the effective number of ultrarelativistic species is larger, and/or decoupling out of LTE with a distribution function that favors *smaller* momenta, thereby making the denominator in Eq. (2.49) smaller, the smaller number of particles allows a larger mass to saturate the DM abundance.

For the particle to be a suitable dark matter candidate, the free-streaming length must be much smaller than the Hubble radius. Although we postpone to a companion article [51] a more detailed study of the free-streaming

lengths in terms of the *generalized distribution functions*, here we adopt the simple requirement that the velocity dispersion be small, namely, the particle must be nonrelativistic

$$\langle \vec{V}^2 \rangle = \left\langle \frac{\vec{P}_T^2}{m^2} \right\rangle \ll 1. \quad (2.50)$$

From Eq. (2.43) this constraint yields

$$\frac{m}{T_d(t)} \gg \sqrt{\frac{\int_0^\infty y^4 f_d(y) dy}{\int_0^\infty y^2 f_d(y) dy}}, \quad (2.51)$$

where $T_d(t)$ is given by Eq. (2.33). From Eqs. (2.13), (2.34), (2.46), and (2.51) we obtain the following condition for the particle to be nonrelativistic at redshift z :

$$m \gg 2.958 \frac{1+z}{g_d^{1/3}} \times 10^{-4} \sqrt{\frac{\int_0^\infty y^4 f_d(y) dy}{\int_0^\infty y^2 f_d(y) dy}} \text{ eV}. \quad (2.52)$$

Taking the relevant value of the redshift for large scale structure to be the redshift at which reionization occurs $z_s \sim 10$ [52], we find the following *generalized* constraint on the mass of the particle of species (a) which is a dark matter component

$$\begin{aligned}\frac{2.958}{g_d^{1/3}} \times 10^{-4} \sqrt{\frac{\int_0^\infty y^4 f_d(y) dy}{\int_0^\infty y^2 f_d(y) dy}} \text{ eV} &\ll m \\ &\leq 2.695 \frac{2g_d \zeta(3)}{g \int_0^\infty y^2 f_d(y) dy} \text{ eV}.\end{aligned}\quad (2.53)$$

The left side of the inequality corresponds to the requirement that the particle be nonrelativistic at reionization (taking $z_s \sim 10$), namely, a small velocity dispersion $\langle \vec{V}^2/c^2 \rangle \ll 1$, corresponding to a free-streaming length $\lambda_{fs} \sim \sqrt{\langle \vec{V}^2/c^2 \rangle} d_H$ much smaller than the Hubble radius (d_H), while the right-hand side is the constraint from the requirement that the decoupled particle is a dark matter *component*, namely, Eq. (2.49) is fulfilled.

III. LIGHT THERMAL RELICS AS DARK MATTER COMPONENTS

In this section we consider particles that decouple in LTE.

A. Fermi-Dirac and noncondensed Bose-Einstein gases of light particles as DM components

The functions $I_\rho(x)$, $I_p(x)$ in the density and pressure denoted by $I_\pm(x)$, $J_\pm(x)$, respectively, for fermions (+) and bosons (−) and the equation of state $w[x]$ [Eq. (2.37)] for each case are depicted in Figs. 1 and 2 for vanishing chemical potential in both cases. We have also numerically studied these functions for values of the chemical potential in the range $0 \leq |\mu_d|/T_d \leq 0.5$ but the difference with the

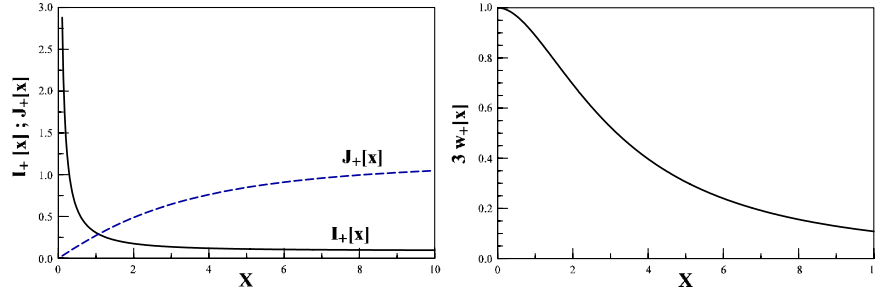


FIG. 1 (color online). Fermions without chemical potential. Left panel: $I_+(x)$ and $J_+(x)$ vs x . Right panel: $3w_+[x]$ vs x . $I_+ = I_\rho$, $J_+ = I_\mathcal{P}$.

case of vanishing chemical potentials is less than $\sim 5\%$ even for the largest value studied $|\mu_d|/T_d = 1.0$ which is about the maximum consistent with constraints on lepton asymmetries allowed by big bang nucleosynthesis (BBN) and CMB [53].

These figures make clear that the onset of the nonrelativistic behavior occurs for $x_{nr} \sim 5$ in both cases. It is useful to compare this result, with the generalized constraint equation (2.51) for the case of thermal relics. Replacing the LTE distribution functions (Fermi-Dirac or Bose-Einstein, without chemical potentials) in Eq. (2.51) we obtain

$$x_{nr} > 3.597 \text{ for fermions,} \quad x_{nr} > 3.217 \text{ for bosons.} \quad (3.1)$$

The detailed analysis of the corresponding functions yields the more precise estimate $x_{nr} \gtrsim 5$ in both cases for the transition to the nonrelativistic regime.

Therefore, the decoupled particle of mass m becomes nonrelativistic at a time t^* when $m \gtrsim 5T_d(t^*)$. At the time of BBN when [32] $T_{\text{BBN}} \sim 0.1$ MeV and $g_{\text{BBN}} \sim 10$, the decoupled particle is nonrelativistic if

$$m \gtrsim g_d^{-(1/3)} \text{ MeV,} \quad (3.2)$$

in which case it does not contribute to the effective number of ultrarelativistic degrees of freedom during BBN and would not affect the primordial abundances of light elements. If the particle remains ultrarelativistic during BBN the total energy density in radiation is [32]

$$\rho_{\text{tot}}(t) = \frac{\pi^2}{30} g_*(t) T_\gamma^4(t) \left[1 + \frac{cg}{g_*(t)} \left(\frac{g_*(t)}{g_d} \right)^{4/3} \right], \quad (3.3)$$

where T_γ is the (LTE) temperature of the fluid, $c = 1(7/8)$ for bosons (fermions), $g_*(t)$ is the effective number of ultrarelativistic degrees of freedom at time t from particles that remain in LTE at this time, and g_d is the effective number of degrees of freedom at decoupling. The second term in Eq. (3.3) is an extra contribution to the effective number of ultrarelativistic degrees of freedom.

At the time of BBN, $g_*(t_{\text{BBN}}) \sim 10$ [32] and early decoupling of the light particle, $g_d \gg g_*(t_{\text{BBN}})$, leads to a negligible contribution to the effective number of ultrarelativistic degrees of freedom well within the current bounds [54]. Therefore, provided that the decoupled particle is *stable*, either for light particles that remain relativistic during (BBN) but that decouple very early on when $g_d \gg 10$ or when the particle's mass $m > 1$ MeV, there is *no* influence on the primordial abundance of light elements and BBN does *not* provide any tight constraints on the particle's mass.

B. A Bose-condensed light particle as a dark matter component

Consider the case of a light bosonic particle, for example, an axion-like-particle. Typical interactions involve two types of processes, inelastic reactions are number-changing processes and contribute to chemical equilibration, while elastic ones distribute energy and momenta of

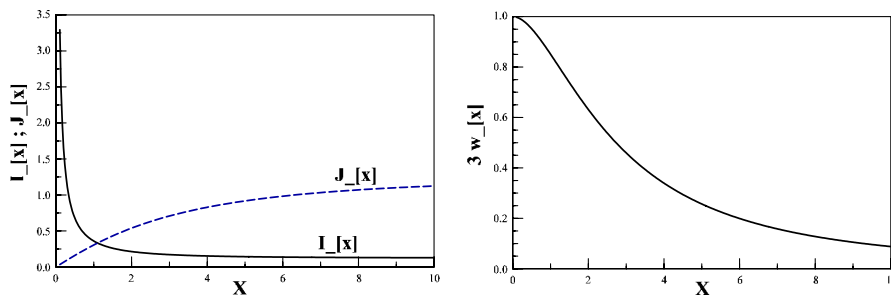


FIG. 2 (color online). Bosons without chemical potential. Left panel: $I_-(x)$ and $J_-(x)$ vs x . Right panel: $3w_-[x]$ vs x . $I_- = I_\rho$, $J_- = I_\mathcal{P}$.

the intervening particles, these do not change the particle number but lead to kinetic equilibration. Consider the case in which chemical freeze-out occurs *before* kinetic freeze-out, such is the case for a real scalar field with quartic self-interactions. In this theory, number-conserving processes such as $2 \rightleftharpoons 2$ establish kinetic (thermal) equilibrium, but conserve particle number, a cross section for such process is $\propto \lambda^2$, where λ is the quartic coupling. The lowest order number-changing processes that contribute to chemical equilibrium are $4 \rightleftharpoons 2$, with cross sections $\propto \lambda^4$. Hence, this is an example of a theory in which chemical freeze-out occurs well before kinetic freeze-out for small coupling.

Another relevant example is the case of WIMPs studied in Ref. [33] where it was found that $T_{cd} \sim 10$ GeV, while $T_{kd} \sim 10$ MeV where T_{cd}, T_{kd} are the chemical and kinetic (thermal) decoupling temperatures, respectively. Although this study focused on a fermionic particle, it is certainly possible that a similar situation, namely, chemical freeze-out much earlier than kinetic freeze-out, may arise for bosonic DM candidates.

Under this circumstance, the number of particles is conserved if the particle is stable, but the temperature continues to redshift by the cosmological expansion, therefore the gas of bosonic particles cools at constant comoving particle number. This situation must eventually lead to Bose-Einstein condensation (BEC) since the thermal distribution function can no longer accommodate the particles with nonvanishing momentum within a thermal distribution. Once thermal freeze-out occurs, the frozen distribution *must* feature a homogeneous condensate and the number of particles for zero momentum becomes macroscopically large. Although some aspects of Bose-Einstein condensates were studied in Refs. [35,36], we study new aspects such as the impact of the BEC upon the bound for the mass and *the velocity dispersion* of DM candidates.

The bosonic distribution function for a fixed number of particles includes a chemical potential and is given by Eq. (2.14) where $\mu_d \leq m$ for the distribution function to be manifestly positive for all p . Separating explicitly the contribution from the $\vec{p} = 0$ mode the number of particles *per comoving volume* V_c is

$$n = \frac{1}{V_c} \frac{1}{e^{(m-\mu_d)/T_d} - 1} + \frac{1}{V_c} \sum_{\vec{p}_c} \frac{1}{e^{(\sqrt{m^2+p_c^2}-\mu_d)/T_d} - 1} \equiv n_0 + \int \frac{d^3 p_c}{(2\pi)^3} \frac{1}{e^{(\sqrt{m^2+p_c^2}-\mu_d)/T_d} - 1}, \quad (3.4)$$

where

$$n_0 = \frac{1}{V_c} \frac{1}{e^{(m-\mu_d)/T_d} - 1} \quad (3.5)$$

is the comoving condensate density. In the infinite volume limit the condensate term vanishes unless $\mu_d \rightarrow m$. For $m/T_d \ll 1$ we find

$$n = n_0 + \frac{T_d^3 \zeta(3)}{\pi^2} Z[e^{\mu_d/T_d}], \quad (3.6)$$

where

$$Z[e^{\mu_d/T_d}] = \frac{1}{\zeta(3)} \sum_l \frac{e^{l\mu_d/T_d}}{l^3}. \quad (3.7)$$

The maximum value that μ_d can achieve is m , therefore, neglecting m/T_d we replace $Z[e^{\mu_d/T_d}]$ by $Z[1] = 1$. If the comoving particle density

$$n > \frac{T_d^3 \zeta(3)}{\pi^2} \quad (3.8)$$

then, there must be a zero momentum condensate with $n_0 \neq 0$ and $\mu_d = m$ in the infinite (comoving) volume limit. In this limit we find

$$1 - \frac{n_0}{n} = \begin{cases} \left(\frac{T_d}{T_c}\right)^3 & \text{for } T_d < T_c \\ 0 & \text{for } T_d > T_c, \end{cases} \quad (3.9)$$

where the critical temperature is given by

$$T_c = \left[\frac{\pi^2 n}{\zeta(3)} \right]^{1/3}. \quad (3.10)$$

The solution of the Eq. (3.4) that determines the condensate fraction shows that for $T_d < T_c$

$$\mu_d = m. \quad (3.11)$$

In the infinite volume limit the distribution function for particles that decouple while ultrarelativistic $m/T_d \ll 1$, for $T_d < T_c$ becomes

$$f_d(p_c) = n_0 \delta^{(3)}(\vec{p}_c) + \frac{1}{e^{p_c/T_d} - 1}. \quad (3.12)$$

From Eq. (2.22) the total number of particles for $m/T_d \ll 1$, $T_c > T_d$ is given by

$$n(t) = n_0(t) + \frac{\zeta(3)}{\pi^2} T_d^3(t), \quad (3.13)$$

where

$$n_0(t) = \frac{n_0}{a^3(t)}. \quad (3.14)$$

For $T_d < T_c$ Eq. (3.9) implies that

$$n_0(t) = \frac{\zeta(3)}{\pi^2} \left[\left(\frac{T_c}{T_d}\right)^3 - 1 \right] T_d^3(t), \quad (3.15)$$

hence for $T_d < T_c$ the total density is given by

$$n(t) = \frac{\zeta(3)}{\pi^2} \left(\frac{T_c}{T_d}\right)^3 T_d^3(t). \quad (3.16)$$

The enhancement factor $(T_c/T_d)^3$ over the thermal result reflects the population of particles in the condensed, zero momentum state. The energy density and pressure are

given by

$$\rho(t) = gm\{n_0(t) + T_d^3(t)I_\rho^{nc}[x(t)]\} \quad (3.17)$$

$$\mathcal{P}(t) = g \frac{T_d^5(t)}{3m} I_{\mathcal{P}}^{nc}[x(t)], \quad (3.18)$$

where

$$I_\rho^{nc}[x(t)] = \frac{1}{2\pi^2} \int_0^\infty \sqrt{1 + \frac{y^2}{x^2(t)}} \frac{y^2}{e^y - 1} dy \quad (3.19)$$

$$I_{\mathcal{P}}^{nc}[x(t)] = \frac{1}{2\pi^2} \int_0^\infty \frac{y^2}{\sqrt{1 + \frac{y^2}{x^2(t)}}} \frac{y^2}{e^y - 1} dy, \quad (3.20)$$

$$x(t) = \frac{m}{T_d(t)}$$

are the contributions from the particles outside the condensate ($p \neq 0$).

Two important aspects emerge from these expressions: (i) *the condensate always contributes as a nonrelativistic component*, (ii) *the condensate does not contribute to the pressure*.

Replacing Eq. (3.15) into (3.17) and using

$$\int_0^\infty \frac{y^2 dy}{e^y - 1} = 2\zeta(3),$$

the energy density and equation of state for $T_d < T_c$ can be written compactly as

$$\rho(t) = gmT_d^3(t)I[x(t)], \quad (3.21)$$

where

$$I[x(t)] = \frac{1}{2\pi^2} \int_0^\infty \left\{ \left[\left(\frac{T_c}{T_d} \right)^3 - 1 \right] + \sqrt{1 + \frac{y^2}{x^2(t)}} \right\} \times \frac{y^2}{e^y - 1} dy. \quad (3.22)$$

The equation of state

$$w[x] = \frac{I_{\mathcal{P}}^{nc}[x]}{3x^2 I[x]} \quad (3.23)$$

is displayed in Fig. 3, from which it is clear that for $T_c/T_d > 1$ the nonrelativistic limit sets in *much earlier* than for the non-Bose-condensed case. This is a consequence of the zero momentum particles in the BEC which contribute as *pressureless* cold matter, even when the light bosonic particle decouples while ultrarelativistic.

For $T_d < T_c$ when the particle becomes nonrelativistic, namely $x \rightarrow \infty$, the energy density becomes

$$\rho(t) = gmn(t), \quad (3.24)$$

where $n(t)$ is the total number of particles per physical volume, including the condensate and noncondensate components, from Eq. (3.16) it follows that

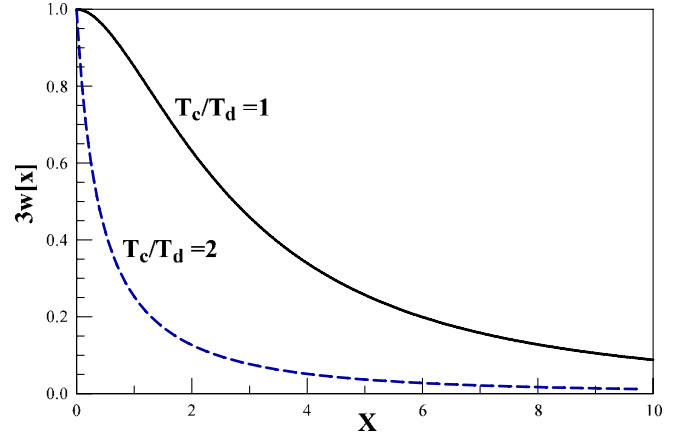


FIG. 3 (color online). $3w[x]$ vs x for the Bose-condensed case for $T_c/T_d = 1-2$.

$$\rho(t) = gm \frac{\zeta(3)}{\pi^2} \left(\frac{T_c}{T_d} \right)^3 T_d^3(t), \quad (3.25)$$

from which for $T_c \geq T_d$ it follows analogously to Eq. (2.47) that

$$\Omega_{\text{BE}} h^2 = \frac{m}{25.67 \text{ eV}} \frac{g}{g_d} \left(\frac{T_c}{T_d} \right)^3. \quad (3.26)$$

The dark matter fraction that these particles can contribute is given by

$$\nu_{\text{BE}} = \frac{m}{2.695 \text{ eV}} \frac{g}{g_d} \left(\frac{T_c}{T_d} \right)^3, \quad (3.27)$$

resulting in the *upper bound*

$$m \leq 2.695 \frac{g_d}{g} \left(\frac{T_d}{T_c} \right)^3 \text{ eV}. \quad (3.28)$$

In the Bose-condensed case $T_d/T_c < 1$ the bosonic particle is light unless it decouples very early on at high temperature with a large g_d . The presence of a BEC *tightens* the constraint on the mass of the light bosonic particle via the extra factor $(T_d/T_c)^3$ in (3.28).

A quantity of importance for clustering is the velocity dispersion when the particle becomes nonrelativistic, it is given by

$$\langle \vec{V}^2 \rangle = \left\langle \frac{\vec{P}_f^2}{m^2} \right\rangle = 12 \frac{\zeta(5)}{\zeta(3)} \left[\frac{T_d(t)}{m} \right]^2 \left(\frac{T_d}{T_c} \right)^3, \quad (3.29)$$

where $\zeta(5) = 1.0369278\dots$

The presence of the BEC, accounted for by the factor $(T_d/T_c)^3 < 1$ in Eq. (3.29), *diminishes* the velocity dispersion. This is a consequence of the fact that the particles in the condensate all have vanishing momentum, and only the noncondensate particles contribute to the velocity dispersion but the fraction of particles outside of the condensate is precisely the factor $(T_d/T_c)^3$. Therefore the presence of a BEC leads to a *decrease* in the velocity dispersion and

consequently *even for light particles to a decrease in the free-streaming length.*

These results imply that, although the bosonic particle is bound to be very light by the bound (3.28) (unless they decoupled very early), if $T_c \gg T_d$ it is *not* a HDM component but can effectively act as either a WDM or CDM because of a *small velocity dispersion*. Whether $T_c \gg T_d$ or not has to be studied within the microscopic particle physics model that describes this DM component.

IV. COARSE GRAINED PHASE-SPACE DENSITIES AND NEW DM BOUNDS

In their seminal article Tremaine and Gunn [30] argued that the coarse grained phase-space density is always smaller than or equal to the maximum of the (fine grained) microscopic phase-space density, which is the distribution function. Such an argument relies on the theorem [43] that states that collisionless phase mixing or violent relaxation by gravitational dynamics can only diminish the coarse grained phase-space density. A similar argument was presented by Dalcanton and Hogan [11,38], and confirmed by recent numerical studies [44].

As noticed in Ref. [36], the case of the Bose-Einstein distribution requires a careful treatment because for massless particles the Bose-Einstein distribution diverges at small momentum. This divergence is present if there is a BEC even when the mass of the bosonic particle is included. This is so since $\mu_d = m$ is required to form a BEC and the distribution functions diverge at zero momentum,

$$\frac{2\pi^2 n_0}{T_d^3} = \begin{cases} 2\zeta(3) \left[\left(\frac{T_c}{T_d} \right)^3 - 1 \right] & \text{for the BEC with } T_d < T_c \\ 0 & \text{for the fermionic or non-Bose condensed case.} \end{cases} \quad (4.3)$$

When the particle becomes nonrelativistic $\rho(t) = mn(t)$ and $\langle \vec{V}^2 \rangle = \langle \frac{P_d^2}{m^2} \rangle$, therefore

$$\mathcal{D} = \frac{\rho}{m^4 \langle \vec{V}^2 \rangle^{3/2}} = \frac{Q_{\text{DH}}}{m^4}, \quad (4.4)$$

where Q_{DH} is the phase-space density introduced by Dalcanton and Hogan [11,38]

$$Q_{\text{DH}} = \frac{\rho}{\langle \vec{V}^2 \rangle^{3/2}}, \quad (4.5)$$

and the one-dimensional velocity dispersion σ is defined by Eq. (2.44).

In the nonrelativistic regime \mathcal{D} is related to the coarse grained phase-space density Q_{TG} introduced by Tremaine and Gunn [30]:

$$Q_{\text{TG}} = \frac{\rho}{m^4 (2\pi\sigma^2)^{3/2}} = \left(\frac{3}{2\pi} \right)^{3/2} \mathcal{D}. \quad (4.6)$$

The observationally accessible quantity is the phase-space density ρ/σ^3 , therefore, using $\rho = mn$ for a decoupled

particle that is nonrelativistic today and Eq. (2.44), we define the primordial phase-space density

even the part of the distribution function that describes the particles outside the condensate diverges at $P = 0$. Madsen recognized this caveat in the bosonic case and in Ref. [36] introduced an alternative *statistical interpretation* of the phase-space density, similar to that introduced in [11,38] but with the upper limit in the momentum integrals replaced by a (physical) momentum cutoff as suggested by the phase mixing theorem [43]. However, it is straightforward to show that the resulting coarse grained phase-space density is *not* a Liouville invariant. Instead, we define the coarse grained (dimensionless) primordial phase-space density

$$\mathcal{D} \equiv \frac{n(t)}{\langle \vec{P}_f^2 \rangle^{3/2}}, \quad (4.1)$$

which is Liouville invariant and where $\langle \vec{P}_f^2 \rangle$ is defined in Eq. (2.49). Since the distribution function is frozen and is a solution of the collisionless Boltzmann (Liouville) equation (2.13), it is clear that \mathcal{D} is a *constant*, namely, a Liouville invariant in absence of self-gravity. Including explicitly a possible BEC, \mathcal{D} is given by

$$\mathcal{D} = \frac{g}{2\pi^2} \frac{[\frac{2\pi^2 n_0}{T_d^3} + \int_0^\infty y^2 f_d(y) dy]^{5/2}}{[\int_0^\infty y^4 f_d(y) dy]^{3/2}}, \quad (4.2)$$

where $f_d(y)$ is the distribution function for the noncondensed particles in the bosonic case and n_0 is the *comoving* density of the Bose-Einstein condensate

particle that is nonrelativistic today and Eq. (2.44), we define the primordial phase-space density

$$\frac{\rho_{\text{DM}}}{\sigma_{\text{DM}}^3} = 3^{3/2} m^4 \mathcal{D} \equiv 6.611 \times 10^8 \mathcal{D} \left[\frac{m}{\text{keV}} \right]^4 \frac{M_\odot/\text{kpc}^3}{(\text{km/s})^3}, \quad (4.7)$$

where we used that $\text{keV}^4 (\text{km/s})^3 = 1.2723 \times 10^8 \frac{M_\odot}{\text{kpc}^3}$.

During collisionless gravitational dynamics, phase mixing increases the density and velocity dispersions in such a way that the coarse grained phase-space density either remains constant or *diminishes*, namely,

$$\frac{\rho}{\sigma^3} \leq 6.611 \times 10^8 \mathcal{D} \left[\frac{m}{\text{keV}} \right]^4 \frac{M_\odot/\text{kpc}^3}{(\text{km/s})^3}, \quad (4.8)$$

where \mathcal{D} is given by Eq. (4.2) for an arbitrary distribution function. For a particle that decouples when it is ultrarelativistic \mathcal{D} does not depend on the mass, hence Eq. (4.8) yields a *lower* bound on the mass of the particle directly

from the observed phase-space density and the knowledge of the distribution function.

For comparison it is convenient to gather the values \mathcal{D} [Eq. (4.2)] for the usual LTE cases that follow from Eqs. (2.31) and (2.35):

$$\mathcal{D} = g \times \begin{cases} 1.963 \times 10^{-3} \text{ fermions, } \mu_d = 0 \\ 3.657 \times 10^{-3} \text{ bosons without BEC} \\ 3.657 \times 10^{-3} \left(\frac{T_c}{T_d}\right)^{15/2} \text{ bosons with BEC, } T_c > T_d \\ 8.442 \times 10^{-2} g_d Y_\infty \text{ nonrelativistic Maxwell-Boltzmann,} \end{cases} \quad (4.9)$$

where g_d is the number of ultrarelativistic degrees of freedom at decoupling.

We note that for $T_c \gg T_d$ the presence of a BEC increases dramatically the primordial phase-space density. This is a consequence of the *enhancement* of the particle density over the thermal case due to the presence of the condensate, and the *decrease* in the velocity dispersion because the particles in the condensate all have zero momentum.

A. New bounds from phase-space density and dShps data

We derive here new bounds from the latest compilation presented in Ref. [14] directly on ρ/σ^3 for the data set comprising ten satellite galaxies in the Milky Way dSphs. It proves convenient to write Eq. (4.8) as

$$m^4 \geq \frac{[62.36 \text{ eV}]^4}{\mathcal{D}} 10^{-4} \frac{\rho}{\sigma^3} \frac{(\text{km/s})^3}{M_\odot/\text{kpc}^3}, \quad (4.10)$$

the data in Ref. [14] yields the range

$$0.9 \leq 10^{-4} \frac{\rho}{\sigma^3} \frac{(\text{km/s})^3}{M_\odot/\text{kpc}^3} \leq 20, \quad (4.11)$$

and we choose a fiducial value for this quantity in the middle of the range of the data [14] ~ 5 – 10 , leading to the new bound

$$m \geq \frac{100}{\mathcal{D}^{1/4}} \text{ eV}. \quad (4.12)$$

For thermal relics that decoupled while ultrarelativistic with vanishing chemical potentials and no BEC, we find from Eqs. (4.9) and (4.12),

$$m \geq \frac{1}{g^{1/4}} \begin{cases} 0.475 \text{ keV fermions} \\ 0.407 \text{ keV bosons without BEC,} \end{cases} \quad (4.13)$$

and for bosons with BEC ($T_d < T_c$) we find

$$m \geq \frac{1}{g^{1/4}} 0.407 \text{ keV} \left[\frac{T_d}{T_c}\right]^{15/8} \text{ bosons with BEC.} \quad (4.14)$$

For particles that decouple *out of LTE* with arbitrary distribution functions the form of the new bound is given by Eq. (4.12) with \mathcal{D} given by Eq. (4.2). The detailed form of \mathcal{D} is completely determined by the distribution function at decoupling, which must be obtained from a microscopic calculation of the kinetics of decoupling. Once the distri-

bution function is obtained, the new bound equation (4.12) yields the *lower bound* of the mass consistent with the observational data.

Combining the *upper bound* (2.49) with the *lower bound* Eq. (4.10) we establish the mass range for the DM candidate

$$\frac{62.36 \text{ eV}}{\mathcal{D}^{1/4}} \left[10^{-4} \frac{\rho}{\sigma^3} \frac{(\text{km/s})^3}{M_\odot/\text{kpc}^3} \right]^{1/4} < m \\ \leq 2.695 \text{ eV} \frac{2g_d \zeta(3)}{g \int_0^\infty y^2 f_d(y) dy}, \quad (4.15)$$

where \mathcal{D} is given by Eq. (4.2) and the compilation of data in [14] constrains the bracket $[\dots]^{1/4} \sim 1$ – 2 .

For thermal relics that decoupled in LTE while ultrarelativistic, and taking the bracket in the middle of the range, we obtain from Eqs. (4.9) and (4.15)

$$\frac{444 \text{ eV}}{g^{1/4}} \leq m \leq \frac{g_d}{g} 4.253 \text{ eV fermions with } \mu_d = 0, \\ \frac{380 \text{ eV}}{g^{1/4}} \leq m \leq \frac{g_d}{g} 2.695 \text{ eV bosons with } \mu_d \\ = 0 \text{ and no BEC}$$

$$\frac{380 \text{ eV}}{g^{1/4}} \left[\frac{T_d}{T_c}\right]^{15/8} \leq m \leq \frac{g_d}{g} 2.695 \left[\frac{T_d}{T_c}\right]^3 \text{ eV BEC.} \quad (4.16)$$

Therefore, if the thermal relic decouples in *equilibrium* this mass range indicates that it *must* decouple when $g_d g^{-(3/4)} > 110$ – 150 , namely, at or above the electroweak scale [32]. In the BEC case, for $T_d \ll T_c$ the fulfillment of the bound requires very large $g_d g^{-(3/4)}$, namely, thermal decoupling at a scale much larger than the electroweak scale.

An alternative is that the particle is very weakly coupled to the plasma and decouples *away* from equilibrium with a distribution function that yields a *smaller abundance* increasing the right-hand side of Eq. (4.16).

B. Generalized Tremaine-Gunn bound

The Tremaine-Gunn bound [30] establishes a relation between the properties of dark matter in galaxies through their phase-space densities. It assumes that dark matter could be reliably described by an isothermal sphere solution of the Lane-Emden equation with the equation of state (2.44) [55,56]. In thermal equilibrium the quantity [56]

$$\eta = \frac{Gm^2 N}{LT} = \frac{2G\rho L^2}{3\sigma^2} \quad (4.17)$$

is bound to be $\eta \lesssim 1.6$ to prevent the gravitational collapse of the gas. Here $V = L^3$ stands for the volume occupied by the gas, N for the number of particles, and $T = \frac{3}{2}m\sigma^2$ for the gas temperature. The length L is similar to the King radius [55]. However, the King radius follows from the singular isothermal sphere solution while L is the characteristic size of a stable isothermal sphere solution [56].

Combining Eq. (4.17) with Eq. (4.8) results in a *generalized* Tremaine-Gunn bound,

$$m^4 \geq \frac{\eta}{2\sqrt{3}GL^2\sigma\mathcal{D}} = \eta \frac{[85.22 \text{ eV}]^4}{\mathcal{D}} \frac{10 \text{ km/s}}{\sigma} \left[\frac{\text{kpc}}{L} \right]^2, \quad (4.18)$$

therefore the *generalized* Tremaine-Gunn bound on the mass becomes

$$m \geq \frac{85.22 \text{ eV}}{\mathcal{D}^{1/4}} \eta^{1/4} \left[\frac{10 \text{ km/s}}{\sigma} \right]^{1/4} \left[\frac{\text{kpc}}{L} \right]^{1/2}. \quad (4.19)$$

The compilation of recent photometric and kinematic data from ten Milky Way dSphs satellites [14] yield values for the one-dimensional velocity dispersion (σ) and the radius (L) in the ranges

$$0.5 \text{ kpc} \leq L \leq 1.8 \text{ kpc}, \quad 6.6 \text{ km/s} \leq \sigma \leq 11.1 \text{ km/s}. \quad (4.20)$$

For particles that decouple in LTE when they are ultrarelativistic (ultrarelativistic thermal relics) with vanishing chemical potential and no BEC, we find from Eqs. (4.9) and (4.19)

$$m \geq \left(\frac{\eta}{g} \right)^{1/4} \left[\frac{10 \text{ km/s}}{\sigma} \right]^{1/4} \times \left[\frac{\text{kpc}}{L} \right]^{1/2} \begin{cases} 0.405 \text{ keV fermions} \\ 0.347 \text{ keV bosons.} \end{cases} \quad (4.21)$$

For the case of ultrarelativistic bosonic thermal relics with a BEC and $T_d < T_c$ we find the bound

$$m \geq \left(\frac{\eta}{g} \right)^{1/4} 0.347 \text{ keV} \left[\frac{10 \text{ km/s}}{\sigma} \right]^{1/4} \left[\frac{\text{kpc}}{L} \right]^{1/2} \left[\frac{T_d}{T_c} \right]^{15/8}. \quad (4.22)$$

Therefore, the BEC case allows for *smaller masses* to saturate the Tremaine-Gunn bound for $T_c \gg T_d$, a consequence of the *enhanced* primordial phase-space density in the presence of the BEC.

C. DM mass values from velocity dispersion

We can use the independent data provided in Ref. [14] on the mean density and velocity dispersion to explore bounds solely from the velocity dispersion. Since the phase-space density only *diminishes or remains constant* during the collisionless gravitational dynamics of cluster-

ing, from which it follows that

$$\frac{\rho_{\text{DM}}}{\sigma_{\text{DM}}^3} \geq \frac{\rho_s}{\sigma_s^3}, \quad (4.23)$$

where ρ_{DM} and σ_{DM} are, respectively, the matter density and velocity dispersion of the *homogeneous* dark matter prior to gravitational collapse. ρ_s and σ_s are, respectively, the satellite's mean volume mass density and velocity dispersion. Assuming that DM has a single component, its density today is [49]

$$\begin{aligned} \rho_{\text{DM}} &= \Omega_{\text{DM}} h^2 1.054 \times 10^4 \text{ eV/cm}^3 \\ &= 1.107 \times 10^3 \text{ eV/cm}^3, \end{aligned} \quad (4.24)$$

σ_{DM} is given by Eq. (2.45). Reference [14] quotes the following values for the favored satellite's cored dark matter density and velocity dispersion:

$$\rho_s \sim 5 \frac{\text{GeV}}{\text{cm}^3}, \quad \sigma_s \sim 10 \frac{\text{km}}{\text{s}}. \quad (4.25)$$

Equations (4.23), (4.24), and (4.25) lead to

$$\sigma_{\text{DM}} \leq 0.06 \frac{\text{km}}{\text{s}}. \quad (4.26)$$

Combining Eq. (2.45) for $z = 0$ and Eq. (4.26) yields

$$\frac{m}{\text{keV}} \geq \frac{0.847}{g_d^{1/3}} \left[\frac{\int_0^\infty y^4 f_d(y) dy}{\int_0^\infty y^2 f_d(y) dy} \right]^{1/2}. \quad (4.27)$$

For thermal fermions or bosons without chemical potential (no BEC) and $10 < g_d \leq 100$, we find $m \sim 0.6\text{--}1.5$ keV in agreement with the bounds found above and the conclusions of Ref. [57]. A suppression factor $(T_d/T_c)^3$ appears in the BEC case for the same range of g_d .

We emphasize that the bound equation (4.27) is *independent* from the bound equation (4.13) obtained from the phase-space density above, and relies on the fact that the observational data [14] yields separate information on ρ_s and σ_s .

It proves illuminating to analyze the velocity dispersion σ_{DM} from expression (2.45) at $z = 0$ for thermal relics. We find

$$\begin{aligned} \sigma_{\text{DM}} &= \frac{1}{g_d^{1/3}} \frac{\text{keV km}}{m \text{ s}} \\ &\times \begin{cases} 0.187 \text{ fermions } \mu_d = 0 \\ 0.167 \text{ bosons no BEC} \\ 0.167 \times \left(\frac{T_d}{T_c} \right)^{3/2} \text{ bosons with BEC, } T_c > T_d \\ 0.09 \times \sqrt{x_d} \text{ nonrelativistic.} \end{cases} \end{aligned} \quad (4.28)$$

We see that for $T_c \gg T_d$ light bosonic particles that decoupled while ultrarelativistic but undergo BEC can effectively act as CDM with *very small* velocity dispersion.

In Ref. [33] it is found that kinetic decoupling for a WIMP of mass $m \sim 100$ GeV occurs at $T_d \sim 10$ MeV, leading to the estimate $\sqrt{x_d} = \sqrt{m/T_d} \sim 100$. Thus, for CDM from weakly interacting massive particles the velocity dispersion equation (4.28) is

$$\sigma_{\text{wimp}} \sim 10^{-8} \left(\frac{100 \text{ GeV}}{m} \right) \frac{\sqrt{x_d}}{100} g_d^{-1/3} \left(9 \frac{\text{km}}{\text{s}} \right). \quad (4.29)$$

Thus, σ_{wimp} is 8 orders of magnitude smaller than the typical velocity dispersion in dSphs [14] for wimps of $m \sim 100$ GeV that decoupled in LTE at $T_d \sim 10$ MeV [33].

It is noteworthy to compare the phase-space densities of the homogeneous dark matter distribution for the thermal relics that decoupled ultrarelativistically and nonrelativistically with that observed in the satellites dSphs. If the distribution of dark matter is cored [14]¹

$$\left(\frac{\rho_s}{\sigma_s^3} \right)_{\text{cored}} \sim 5 \times 10^6 \frac{\text{eV/cm}^3}{(\text{km/s})^3}. \quad (4.30)$$

If the distribution of dark matter is cusped, Ref. [14] gives the value for the density $\rho_s \sim 2$ TeV/cm³ yielding

$$\left(\frac{\rho_s}{\sigma_s^3} \right)_{\text{cusped}} \sim 2 \times 10^9 \frac{\text{eV/cm}^3}{(\text{km/s})^3}. \quad (4.31)$$

Assuming that a thermal relic that decoupled when ultrarelativistic is the *only* DM component with the density given by the value today $\rho_{\text{DM}} \sim 1.107 \times 10^3$ eV/cm³ [49], we find from Eqs. (2.45) at $z = 0$,

$$\frac{\rho_{\text{DM}}}{\sigma_{\text{DM}}^3} \sim 10^6 \frac{\text{eV/cm}^3}{(\text{km/s})^3} \left(\frac{m}{\text{keV}} \right)^3 \times g_d \begin{cases} 0.177 \text{ fermions} \\ 0.247 \text{ bosons without BEC} \\ 0.247 (T_c/T_d)^{9/2} \text{ bosons with BEC.} \end{cases} \quad (4.32)$$

Thus, for $g_d > 10$ we see that for $m \sim \text{keV}$ the phase-space density for thermal relics that decoupled being ultrarelativistic is of the *same order* as the phase-space density in dSphs with cores, Eq. (4.30). Thermal relics with mass in the $\sim \text{keV}$ range obviously favor *cores* over *cusps* because the primordial phase space is $\rho_{\text{DM}}/\sigma_{\text{DM}}^3 \geq \rho_s/\sigma_s^3$ for cores while $\rho_{\text{DM}}/\sigma_{\text{DM}}^3 \ll \rho_s/\sigma_s^3$ for a cuspy distribution, and according to the theorem in [30,43], the phase-space density can only diminish during gravitational clustering.

An enhancement factor $(T_c/T_d)^{9/2}$ appears in Eq. (4.32) for the case of a BEC. Notice that, for $T_c/T_d \geq 10$ and $m \sim \text{keV}$, a BEC yields a phase-space density consistent with *cusps* as a result of the *small* velocity dispersion and the CDM behavior.

Recent N -body simulations [44] indicate that the phase-space density decreases by a factor 10 – 10^2 due to gravita-

tional relaxation during structure formation between $0 \leq z \leq 10$, with smaller relaxation in WDM than in CDM [11,44]. Therefore, from these numerical results it follows that

$$\frac{\rho_s}{\sigma_s^3} \sim 10^{-2} \frac{\rho_{\text{DM}}}{\sigma_{\text{DM}}^3}. \quad (4.33)$$

Combining this result with the observational results equations (4.30) and (4.31) and the primordial phase-space density equation (4.32) for a *thermal relic* that decoupled while ultrarelativistic, we find

$$m_{\text{cored}} \sim \frac{15}{g_d^{1/3}} \text{ keV}, \quad m_{\text{cusp}} \sim \frac{100}{g_d^{1/3}} \text{ keV}. \quad (4.34)$$

These values and the *upper* bounds for m in Eqs. (4.16) yield the following bounds for *thermal relics*:

$$\begin{aligned} g_d g^{-(3/4)} &\geq 500 \text{ for cores,} \\ g_d g^{-(3/4)} &\geq 2000 \text{ for cusps.} \end{aligned} \quad (4.35)$$

Therefore, *thermal relics*, DM candidates that decouple when relativistic, must decouple at a temperature well *above* the electroweak scale. Equations (4.34) and (4.35) imply for the mass value:

$$m_{\text{cored}} \sim \frac{2}{g^{1/4}} \text{ keV}, \quad m_{\text{cusp}} \sim \frac{8}{g^{1/4}} \text{ keV}. \quad (4.36)$$

Although m_{cusp} is not too much larger than m_{cored} it is noteworthy that the thermal relic DM candidate that leads to cusped profiles must decouple when $g_d \geq 2000$, namely, very early at a temperature scale corresponding to a grand unified theory with a large symmetry group.

For the case of CDM from wimps which decoupled nonrelativistic, we find from Eqs. (4.24) and (4.28)

$$\frac{\rho_{\text{wimp}}}{\sigma_{\text{wimp}}^3} \sim 10^{24} \frac{\text{eV/cm}^3}{(\text{km/s})^3} \left(\frac{m}{100 \text{ GeV}} \right)^3 \left(\frac{100}{\sqrt{x_d}} \right)^3 g_d. \quad (4.37)$$

The phase-space density always decreases by dynamical relaxation, a result recently confirmed numerically by N -body simulations [44]. For initial values of the phase-space density which are much lower than the primordial ones, these yield a typical decrease by a factor 10^2 – 10^3 [44]. If these results should persist in N -body simulations with larger values of the initial phase-space density, they would imply a tension between the phase-space density of WIMPs equation (4.37) being 18 to 15 orders of magnitude larger than that in dSphs either cored equation (4.30) or cusped equation (4.31) [14].

Combining Eqs. (4.30), (4.31), (4.33), and (4.37) yield for wimps as DM,

$$\begin{aligned} \sqrt{mT_d} &\sim \frac{10}{g_d^{1/3}} \text{ keV for cores,} \\ \sqrt{mT_d} &\sim \frac{100}{g_d^{1/3}} \text{ keV for cusps.} \end{aligned} \quad (4.38)$$

¹(eV/c²)/cm³ = 0.026M_⊙/kpc³.

From the combined analysis of the primordial phase-space densities, the observational data on dSphs [14] and the N -body simulations in Ref. [44], we conclude the following:

- (i) Thermal relics with $m \sim \text{few keV}$ that decouple when ultrarelativistic lead to a primordial phase-space density of the same order of magnitude as in cored dSphs and disfavor cusped satellites for which the data [14] yields a much larger phase-space density.
- (ii) Light bosonic particles decoupled while ultrarelativistic and which form a BEC lead to phase-space densities consistent with cores and if $T_c/T_d \gtrsim 10$, also consistent with cusps. However, for thermal relics to satisfy the bound equation (4.16), they must decouple when $g_d g^{-(3/4)} (T_d/T_c)^{9/8} > 130$, namely, above the electroweak scale. Recall that typically g takes a value between one and four.

V. NONEQUILIBRIUM EFFECTS

The main results of our analysis are the new bounds from DM abundance and phase-space density of dSphs summarized in Eq. (4.15). When the dark matter candidate decouples *out of LTE*, these bounds establish a direct connection with the *microphysics* via the frozen distribution functions. These functions must be obtained from a detailed calculation of the *microscopic processes* that describe the production and pathway towards equilibration of the corresponding dark matter candidate. If kinetic (and chemical) freeze-out occurs out of LTE, the distribution functions will keep memory of the initial state and the detail of the processes that established it.

Nonequilibrium effects have been mainly considered for massive particles that decoupled when nonrelativistic [58] or as distortions in the neutrino distribution functions during BBN [59,60]. Instead, we focus here on DM constraints from decoupling out of (LTE) at temperatures larger than the BBN scale and when particles are ultrarelativistic. *Decoupling out of LTE* in this case has been much less studied. In this section we explore a cosmologically relevant mechanism of production and equilibration which describes a wide variety of situations out of LTE.

A. Particle production followed by an UV cascade

Early studies of particle production via parametric amplification and oscillations of inflatonlike scalar fields revealed that particles are produced via this mechanism primarily in a low momentum band of wave vectors [45] leading to a nonthermal spectrum (Figs. 2–3 in Ref. [45] illustrate these effects).

Subsequent studies [46] showed that the early phase of parametric amplification and particle production is followed by a long stage of mode mixing and scattering that redistributes the particles: the larger momentum modes are populated by a *cascade* whose front moves towards the

ultraviolet akin to a direct cascade in turbulence, leaving in its wake a state of nearly LTE but with a *lower* temperature than that of equilibrium [46].

The dynamics during the cascade process diminishes the amplitude of the distribution function at lower momenta and populates the higher momentum modes. The distribution function develops a *front* that moves towards the ultraviolet. Behind the front the distribution function is nearly that of LTE with a different temperature and amplitude and slowly evolves towards thermal equilibrium [46]. If these particles are very weakly coupled to the plasma, it is possible that the advance of the cascade and the front of the distribution towards larger momenta is *interrupted* when the rate of scattering or mode mixing becomes smaller than the expansion rate. In this case, the distribution function is *frozen* well before reaching complete LTE resulting in a population of modes primarily at lower momenta up to the scale of the front. This study [46] suggests the following frozen distribution function:

$$f_d(y) = f_0 f_{\text{eq}}\left(\frac{y}{\xi}\right) \theta(y_0 - y), \quad (5.1)$$

where $f_{\text{eq}}\left(\frac{p_c}{\xi T_d}\right)$ is the equilibrium distribution function for an ultrarelativistic particle at an effective temperature ξT_d . Namely, $\xi = 1$ at thermal equilibrium and $\xi < 1$ *before* thermodynamical equilibrium is attained.

This form describes fairly accurately the cascade with a *front* that moves towards the ultraviolet, which is *interrupted* at a fixed value of the momentum, identified here to be $p_c^0 = y_0 T_d$; T_d is the temperature of the environmental degrees of freedom that are in LTE at the time of decoupling.

The amplitude f_0 and effective temperature $\xi T_d \leq T_d$ reflect an incomplete thermalization behind the front of the cascade and determine the average number of particles in its *wake* [46]. This interpretation is borne out by the detailed numerical studies in Ref. [46]. For Fermi-Dirac ultrarelativistic particles (with vanishing chemical potential) $0 \leq f_0 \leq 2$, whereas for Bose-Einstein ultrarelativistic particles $0 \leq f_0 \leq \infty$. Neglecting the possibility of a BEC, for a fermionic or bosonic equilibrium distribution function f_{eq} , we find

$$\begin{aligned} \int_0^\infty y^2 f_d(y) dy &= f_0 \xi^3 F\left[\frac{p_c^0}{\xi T_d}\right], \\ F(s) &= \int_0^s y^2 f_{\text{eq}}(y) dy, \\ \int_0^\infty y^4 f_d(y) dy &= f_0 \xi^5 G\left[\frac{p_c^0}{\xi T_d}\right], \\ G(s) &= \int_0^s y^4 f_{\text{eq}}(y) dy, \end{aligned} \quad (5.2)$$

and the primordial phase-space density becomes

$$\mathcal{D} = f_0 \mathcal{D}_{\text{eq}} H(s), \quad s = \frac{y_0}{\xi} = \frac{p_c^0}{\xi T_d}, \quad (5.3)$$

$$H(s) \equiv \left[\frac{F(s)}{F(\infty)} \right]^{5/2} \left[\frac{G(\infty)}{G(s)} \right]^{3/2},$$

where \mathcal{D}_{eq} is the phase-space density equation (4.2) for the equilibrium distribution f_{eq} .

For a fermionic species without chemical potential [$f_{\text{eq}}(y) = 1/(e^y + 1)$], the bound equation (4.15) becomes

$$\frac{475 \text{ eV}}{[f_0 g H(s)]^{1/4}} \leq m \leq \frac{g_d}{g} \frac{4.253}{f_0 \xi^3 F(s)} \text{ eV}, \quad (5.4)$$

and the one-dimensional velocity dispersion equation (2.45) becomes today

$$\sigma_{\text{DM}} = \frac{0.05124 \xi}{g_d^{1/3}} v(s) \left(\frac{\text{keV}}{m} \right) \left(\frac{\text{km}}{s} \right), \quad v(s) \equiv \sqrt{\frac{G(s)}{F(s)}}. \quad (5.5)$$

The functions $F(s)$, $H(s)$, and $v(s)$ for the case $f_{\text{eq}}(y) = 1/(e^y + 1)$ are displayed in Fig. 4. For the Bose-Einstein case without a BEC the behaviors of $F(s)$, $H(s)$, and $v(s)$ are qualitatively similar.

It is clear that the bound equation (5.4) for the range of m can easily be satisfied for moderate values $g_d \sim 10\text{--}50$ corresponding to decoupling temperatures $1 \text{ MeV} \lesssim T_d \lesssim 1 \text{ GeV}$ and $f_0 \xi^3 F(s) \lesssim 0.08$.

Remarkably, the nonequilibrium distribution equation (5.1) turns out to be a generalization of several nonequilibrium distribution functions of cosmological relevance proposed in the literature:

- (a) sterile neutrinos produced nonresonantly via the Dodelson-Widrow mechanism [18] for which the distribution function is obtained from (5.1) by taking $\xi = 1$; $s \rightarrow \infty$, $f_0 \sim 0.043 \text{ keV}/m$ (Ref. [18]). In this case we find for the mass range, phase-space density, and velocity dispersion, respectively:

$$\frac{1.04 \text{ keV}}{g^{1/4}} \leq m \leq \frac{g_d}{g} 56.5 \text{ eV},$$

$$\frac{\rho_{\text{DM}}}{\sigma_{\text{DM}}^3} = 5.7 g \times 10^4 \left[\frac{m}{\text{keV}} \right]^3 \frac{M_\odot/\text{kpc}^3}{(\text{km}/s)^3}, \quad (5.6)$$

$$\sigma_{\text{DM}} = \frac{0.187}{g_d^{1/3}} \left(\frac{\text{keV}}{m} \right) \left(\frac{\text{km}}{s} \right).$$

The major uncertainty is the evaluation of g_d . In the Dodelson-Widrow [18] scenario, the sterile neutrino production peaks at $T \sim 130 \text{ MeV}$, this temperature is very near the region where the QCD phase transition occurs at which the effective number of ultra-relativistic degrees of freedom changes dramatically. If decoupling occurs at a temperature higher than the QCD critical temperature, then $g_d \sim 30$ and the mass bound equation (5.6) may be fulfilled, but for a lower decoupling temperature when $g_d \lesssim 25\text{--}30$ the mass bound may not be fulfilled. If the mass bound is fulfilled, $\rho_{\text{DM}}/\sigma_{\text{DM}}^3$ is compatible with cored dSphs [14] [see Eq. (4.30)] but not with the cusped distributions [see Eq. (4.31)]. Combining the bound equation (5.6), the observed phase-space density equation (4.30) [14], and the N -body results of Ref. [44] which yield phase-space relaxation by a factor $\sim 10^2$, we find that

$$m \sim \frac{4}{g^{1/3}} \text{ keV}. \quad (5.7)$$

- (b) sterile neutrinos produced by a net-lepton number driven resonant conversion studied by Shi and Fuller [19] for which the distribution function is obtained from Eq. (5.1) for $\xi = 1$, $s \sim 0.7$, $f_0 \sim 1$ (see Fig. 1 in the first reference in [19]). We find

$$\frac{289 \text{ eV}}{g^{1/4}} \leq m \leq \frac{g_d}{g} 98.9 \text{ eV},$$

$$\frac{\rho_{\text{DM}}}{\sigma_{\text{DM}}^3} = 9.6 g \times 10^6 \left[\frac{m}{\text{keV}} \right]^4 \frac{M_\odot/\text{kpc}^3}{(\text{km}/s)^3},$$

$$\sigma_{\text{DM}} = \frac{0.028 \text{ keV km}}{g_d^{1/3}} \frac{1}{m} \frac{1}{s}. \quad (5.8)$$

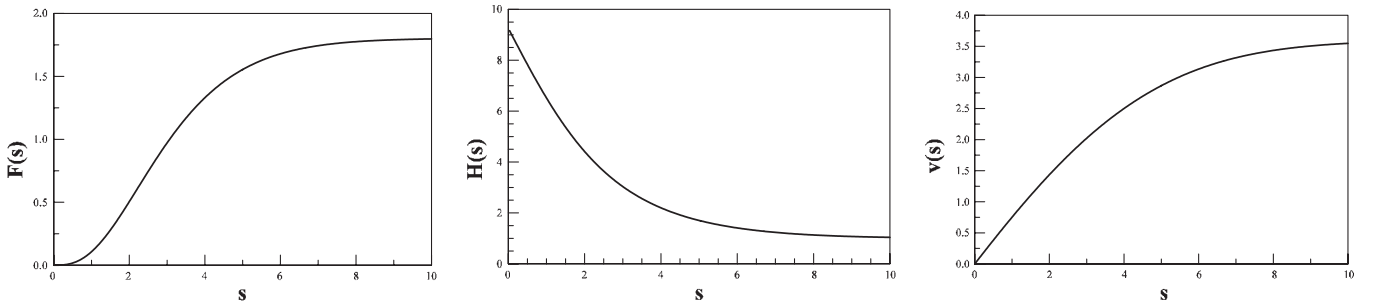


FIG. 4. The functions $F(s)$ (left panel), $H(s)$ (middle panel), and $v(s)$ (right panel) vs $s = y_0/\xi$, for f_{eq} the Fermi-Dirac distribution function without chemical potential.

Again, a source of uncertainty is the evaluation of g_d , because in the resonant-mediated sterile neutrino production, the maximum production rate is near the QCD temperature [19]. However, it is clear that in this case the mass bound is *less sensitive* to the uncertainty in g_d (a small value $g_d \sim 10$ fulfills the bound), although the MSW resonance occurs also near the QCD critical temperature [19]. The velocity dispersion is small because the distribution is skewed towards small momenta. Again, $\rho_{\text{DM}}/\sigma_{\text{DM}}^3$ is consistent with *cored* dSphs [see Eq. (4.30)] but not with *cusped* distributions [see Eq. (4.31)]. A similar analysis as in the previous case combining the observational data, the results of Ref. [44], and the bound Eq. (5.8) yields

$$m \sim \frac{0.8}{g^{1/4}} \text{ keV}. \quad (5.9)$$

- (c) Our distribution function equation (5.1) for $\xi = 1$; $s \rightarrow \infty$ and $f_0 = \beta$ yields the distribution function proposed in Ref. [26] to model WDM [Eq. (8) in Ref. [26]]. We find

$$\begin{aligned} \frac{475 \text{ eV}}{(\beta g)^{1/4}} &\leq m \leq \frac{g_d}{\beta g} 2.36 \text{ eV}, \\ \frac{\rho_{\text{DM}}}{\sigma_{\text{DM}}^3} &= 1.33 \beta g \times 10^6 \left[\frac{m}{\text{keV}} \right]^4 \frac{M_{\odot}/\text{kpc}^3}{(\text{km/s})^3}, \\ \sigma_{\text{DM}} &= \frac{0.187 \text{ keV km}}{g_d^{1/3} m s}. \end{aligned} \quad (5.10)$$

The parameter β cannot be too small, although a small β increases the mass, it decreases the phase-space density.

Although recent studies [61] suggest that the description of the production mechanism of sterile neutrinos must be reassessed with likely implications on their distribution functions after decoupling, the above estimates provide a *guidance* to the range of mass, primordial phase-space density, and velocity dispersions for sterile neutrinos as possible WDM candidates.

VI. CONCLUSIONS

We have obtained new constraints on light DM candidates that decoupled while ultrarelativistic in or out of LTE

in terms of their distribution functions. The only assumption is that these distribution functions are homogeneous and isotropic. A Liouville invariant coarse grained primordial phase-space density is introduced that allows one to combine phase-space density arguments with a recent compilation of photometric and kinematic data on dSphs galaxies to yield *new constraints* on the mass, velocity dispersion, and phase-space density of DM candidates. The new constraint on the mass range is

$$\begin{aligned} \frac{62.36 \text{ eV}}{\mathcal{D}^{1/4}} \left[10^{-4} \frac{\rho}{\sigma^3} \frac{(\text{km/s})^3}{M_{\odot}/\text{kpc}^3} \right]^{1/4} &\leq m \\ &\leq 2.695 \frac{2g_d \xi(3)}{g \int_0^{\infty} y^2 f_d(y) dy} \text{ eV}, \end{aligned} \quad (6.1)$$

where the primordial phase-space density is given by

$$\mathcal{D} = \frac{g}{2\pi^2} \frac{[\int_0^{\infty} y^2 f_d(y) dy]^{5/2}}{[\int_0^{\infty} y^4 f_d(y) dy]^{3/2}}, \quad (6.2)$$

$f_d(p_c/T_d)$ is the distribution function at decoupling, g the number of internal degrees of freedom of the particle, and ρ/σ^3 is the phase-space density obtained from observations. The *upper bound* arises from requesting that the DM candidate has a density $\leq \rho_{\text{DM}}$ today, and the *lower bound* arises from requesting that the phase-space density in halos ρ/σ^3 be *smaller* than or equal to the primordial phase-space density of the collisionless nonrelativistic (today) DM component

$$\rho_{\text{DM}}/\sigma_{\text{DM}}^3 = 3^{3/2} m^4 \mathcal{D}.$$

We have studied the consequences of Bose-Einstein condensation of light ultrarelativistic particles when chemical freeze-out occurs well before kinetic decoupling at $T_d < T_c$ with T_c the critical temperature below which a non-vanishing condensate fraction exists. We find that the presence of the condensate hastens the onset of the nonrelativistic regime and that Bose-Einstein condensed particles can effectively act as a CDM component *even* when they decoupled being ultrarelativistic. The reason for this unusual behavior is that the particles in the condensate all have vanishing velocity dispersion.

For *thermal relics* we find

$$\mathcal{D} = g \times \begin{cases} 1.963 \times 10^{-3} \text{ fermions, } \mu_d = 0 \\ 3.657 \times 10^{-3} \text{ bosons no BEC} \\ 3.657 \times 10^{-3} (T_c/T_d)^{15/2} \text{ bosons with BEC, } T_c > T_d \\ 8.442 \times 10^{-2} g_d Y_{\infty} \text{ nonrelativistic Maxwell-Boltzmann.} \end{cases} \quad (6.3)$$

The combination of data in Ref. [14] from dSphs when applied to *light thermal relics* yields the mass range

$$\begin{aligned} \frac{444 \text{ eV}}{g^{1/4}} &\leq m \leq \frac{g_d}{g} 4.253 \text{ eV fermions with } \mu_d = 0, \\ \frac{380 \text{ eV}}{g^{1/4}} &\leq m \leq \frac{g_d}{g} 2.695 \text{ eV bosons with } \mu_d \\ &= 0 \text{ and no BEC,} \\ \frac{380 \text{ eV}}{g^{1/4}} \left[\frac{T_d}{T_c} \right]^{15/8} &\leq m \leq \frac{g_d}{g} 2.695 \left[\frac{T_d}{T_c} \right]^3 \text{ eV BEC.} \end{aligned} \quad (6.4)$$

with the implication that, if these particles are suitable DM candidates, they must decouple at high temperature when the effective number of ultrarelativistic degrees of freedom is $g_d > 100$. Namely, in absence of a BEC, thermal decoupling must occur above the electroweak scale. In the BEC case, for $T_d \ll T_c$, the fulfillment of the bound requires very large g_d . Namely, in the presence of a BEC thermal decoupling occurs at a scale much larger than the electroweak scale for $T_d \ll T_c$.

Assuming that the DM particle is the only component with the density ρ_{DM} today, we obtained an independent bound from velocity dispersion which for the favored cored profiles [14] yield the lower mass bound,

$$\frac{m}{\text{keV}} \geq \frac{0.855}{g_d^{1/3}} \left[\frac{\int_0^\infty y^4 f_d(y) dy}{\int_0^\infty y^2 f_d(y) dy} \right]^{1/2}. \quad (6.5)$$

For light thermal relics this bound implies that $m \geq 0.6\text{--}1.5$ keV with a suppression factor T_d/T_c in the BEC case.

For light thermal relics that decoupled while ultrarelativistic, we find the primordial phase-space density

$$\begin{aligned} \frac{\rho_{\text{DM}}}{\sigma_{\text{DM}}^3} &\sim 10^6 \frac{\text{eV/cm}^3}{(\text{km/s})^3} \left(\frac{m}{\text{keV}} \right)^3 \\ &\times g_d \begin{cases} 0.177 \text{ fermions} \\ 0.247 \text{ bosons without BEC} \\ 0.247 (T_c/T_d)^{9/2} \text{ bosons with BEC.} \end{cases} \end{aligned} \quad (6.6)$$

An enhancement factor $(T_c/T_d)^{9/2}$ appears in the right-hand side in the presence of a BEC.

For wimps with kinetic decoupling temperature 10 MeV [33], we find

$$\frac{\rho_{\text{wimp}}}{\sigma_{\text{wimp}}^3} \sim 10^{24} \frac{\text{eV/cm}^3}{(\text{km/s})^3} \left(\frac{m}{100 \text{ GeV}} \right)^3 g_d. \quad (6.7)$$

The observational data compiled in Ref. [14] assuming a favored cored profile suggests

$$\left(\frac{\rho_s}{\sigma_s^3} \right)_{\text{cored}} \sim 5 \times 10^6 \frac{\text{eV/cm}^3}{(\text{km/s})^3}. \quad (6.8)$$

If the distribution of dark matter is cusped, Ref. [14] gives the value for the density $\rho_s \sim 2 \text{ TeV/cm}^3$ yielding

$$\left(\frac{\rho_s}{\sigma_s^3} \right)_{\text{cusped}} \sim 2 \times 10^9 \frac{\text{eV/cm}^3}{(\text{km/s})^3}. \quad (6.9)$$

Therefore, for $g_d \geq 10$ the primordial phase-space density for *thermal relics* with $m \sim \text{keV}$ favors a *cored distribution*.

Notice that a bosonic thermal relic that features a BEC can behave as CDM with small velocity dispersion and a primordial phase-space density consistent with cusped distributions if $T_d \ll T_c$. However, these BEC DM candidates must decouple at a temperature scale *higher* than the electroweak.

Recent results from N -body simulations suggests that the phase-space density relaxes by a factor $\sim 10^2$ during gravitational clustering for $0 \leq z \leq 10$ [44]. Combining these numerical results with the observational results on dSphs [14] and the present DM density, we conclude that the mass of *thermal relics* that decoupled when ultrarelativistic is

$$m_{\text{cored}} \sim \frac{2}{g^{1/4}} \text{ keV}, \quad m_{\text{cusped}} \sim \frac{8}{g^{1/4}} \text{ keV}. \quad (6.10)$$

The decoupling temperature for the DM candidate that would favor cusped profiles must be near a grand unified scale for a large symmetry group with $g_d \geq 2000$ which effectively results in a colder relic today with a far smaller velocity dispersion.

The *enormous* discrepancy between the primordial phase-space density for WIMPs of $m \sim 100 \text{ GeV}$; $T_d \sim 10 \text{ MeV}$, Eq. (6.7), and the phase-space densities in dSphs, either cored [Eq. (6.8)] or cusped [Eq. (6.9)] cannot be explained by the 2 orders of magnitude of gravitational relaxation of phase-space densities found with recent N -body simulations [44], although these initialize the simulation with much smaller values of the primordial phase-space density.

We have studied a scenario for decoupling out of equilibrium motivated by previous studies of particle production and thermalization via an UV cascade. The distribution function obtained from previous studies [46] remarkably describes the nonequilibrium distribution functions for sterile neutrinos produced either resonantly [19] or nonresonantly [18] as well as a recently proposed model for halo structure [26]. Our bounds in terms of arbitrary distribution functions lead to the following bounds on the mass, phase-space density, and velocity dispersion of these light relics that decoupled out of LTE:

- (i) For sterile neutrinos produced nonresonantly via the Dodelson-Widrow mechanism [18], we find

$$\begin{aligned} \frac{1.04 \text{ keV}}{g^{1/4}} &\leq m \leq \frac{g_d}{g} 46.5 \text{ eV,} \\ \frac{\rho_{\text{DM}}}{\sigma_{\text{DM}}^3} &= 0.57 g \times 10^5 \left[\frac{m}{\text{keV}} \right]^3 \frac{M_\odot/\text{kpc}^3}{(\text{km/s})^3}, \\ \sigma_{\text{DM}} &= \frac{0.187}{g_d^{1/3}} \left(\frac{\text{keV}}{m} \right) \left(\frac{\text{km}}{s} \right). \end{aligned} \quad (6.11)$$

The upper and lower bound on the mass can only be

compatible if the sterile neutrino decouples with $g_d \gtrsim 20\text{--}30$. For $m \sim \text{keV}$ the primordial phase-space density is compatible with cored but not with cusped profiles in the dSphs data [14]. Combining these bounds with the results from N -body simulations on the relaxation of the phase-space density [44] and with the observational constraint equation (4.30) [14], we obtain the value

$$m \sim \frac{4}{g^{1/3}} \text{ keV} \quad (6.12)$$

for the mass of sterile neutrinos produced nonresonantly by the Dodelson-Widrow mechanism.

- (ii) For sterile neutrinos produced by a net-lepton number driven resonant conversion [19], we find

$$\begin{aligned} \frac{289 \text{ eV}}{g^{1/4}} &\leq m \leq \frac{g_d}{g} 81.4 \text{ eV}, \\ \frac{\rho_{\text{DM}}}{\sigma_{\text{DM}}^3} &= 9.6g \times 10^6 \left[\frac{m}{\text{keV}} \right]^4 \frac{M_\odot/\text{kpc}^3}{(\text{km/s})^3}, \\ \sigma_{\text{DM}} &= \frac{0.028}{g_d^{1/3}} \left(\frac{\text{keV}}{m} \right) \left(\frac{\text{km}}{s} \right). \end{aligned} \quad (6.13)$$

The small velocity dispersion is a consequence of the distribution function being skewed towards small momentum. Again for $m \sim \text{keV}$, the primordial phase-space density is compatible with cored but not cusped profiles in the dSphs data [14]. For sterile neutrinos produced by resonant conversion, a similar analysis as for the previous case yields

$$m \sim \frac{0.8}{g^{1/4}} \text{ keV}. \quad (6.14)$$

- (iii) For the model proposed in Ref. [26], we find

$$\begin{aligned} \frac{475 \text{ eV}}{(\beta g)^{1/4}} &\leq m \leq \frac{g_d}{\beta g} 1.94 \text{ eV}, \\ \frac{\rho_{\text{DM}}}{\sigma_{\text{DM}}^3} &= 1.33\beta g \times 10^6 \left[\frac{m}{\text{keV}} \right]^4 \frac{M_\odot/\text{kpc}^3}{(\text{km/s})^3}, \\ \sigma_{\text{DM}} &= \frac{0.187}{g_d^{1/3}} \left(\frac{\text{keV}}{m} \right) \left(\frac{\text{km}}{s} \right). \end{aligned} \quad (6.15)$$

It is noteworthy that the N -body results of Ref. [44], which yield phase-space relaxation by a factor $\sim 10^2$, bring the values of the primordial phase-space density of the above cases within the range consistent with the phase-space densities for cored profiles in dSphs [14] for $m \sim \text{keV}$. On the contrary, in the case of WIMPs with $m \sim 100 \text{ GeV}$, $T_d \sim 10 \text{ MeV}$ relaxation by *many* orders of magnitude is necessary for their phase-space densities to be compatible with the observed values both for cores and for cusps.

Therefore the bounds equations (6.12), (6.13), and (6.14) confirm that $\sim \text{keV}$ relics that decouple out of equilibrium while ultrarelativistic via the mechanisms described above yield values for phase-space densities that are in agreement with cores in the DM distribution.

The results obtained in this article for the new mass bounds, primordial phase-space densities and velocity dispersion in terms of arbitrary, but homogeneous and isotropic distribution functions establish a link between the microphysics of decoupling and observable quantities. They also warrant deeper scrutiny of the nonequilibrium aspects of sterile neutrinos [61] for a firmer assessment of their potential as DM candidates.

ACKNOWLEDGMENTS

We thank Carlos Frenk, for useful discussions, D. B. thanks Andrew Zentner for fruitful discussions, and acknowledges support from the U.S. National Science Foundation through Grant No. PHY-0553418.

-
- [1] F. Zwicky, *Helv. Phys. Acta* **6**, 124 (1933); *Phys. Rev.* **51**, 290 (1937); J. H. Oort, *Astrophys. J.* **91**, 273 (1940).
 [2] See, for example, J. Primack, *New Astron. Rev.* **49**, 25 (2005); *Nucl. Phys. B, Proc. Suppl.* **173**, 1 (2007), and references therein.
 [3] G. Kauffman, S. D. M. White, and B. Guiderdoni, *Mon. Not. R. Astron. Soc.* **264**, 201 (1993).
 [4] S. Ghigna *et al.*, *Astrophys. J.* **544**, 616 (2000).
 [5] B. Moore *et al.*, *Astrophys. J. Lett.* **524**, L19 (1999).
 [6] A. Klypin *et al.*, *Astrophys. J.* **523**, 32 (1999).
 [7] J. Dubinski and R. Carlberg, *Astrophys. J.* **378**, 496 (1991).
 [8] J. F. Navarro, C. S. Frenk, and S. White, *Mon. Not. R. Astron. Soc.* **462**, 563 (1996).
 [9] J. S. Bullock *et al.*, *Mon. Not. R. Astron. Soc.* **321**, 559 (2001); A. R. Zentner and J. S. Bullock, *Phys. Rev. D* **66**, 043003 (2002); *Astrophys. J.* **598**, 49 (2003).
 [10] J. Diemand *et al.*, *Mon. Not. R. Astron. Soc.* **364**, 665 (2005).
 [11] J. J. Dalcanton and C. J. Hogan, *Astrophys. J.* **561**, 35 (2001).
 [12] F. C. van den Bosch and R. A. Swaters, *Mon. Not. R. Astron. Soc.* **325**, 1017 (2001).
 [13] R. A. Swaters *et al.*, *Astrophys. J.* **583**, 732 (2003).
 [14] R. F. G. Wyse and G. Gilmore, arXiv:0708.1492; G. Gilmore *et al.*, arXiv:astro-ph/0703308.
 [15] O. E. Gerhard and D. N. Spergel, *Astrophys. J.* **389**, L9 (1992).

- [16] F. C. van den Bosch *et al.*, *Astron. J.* **119**, 1579 (2000).
- [17] B. Moore *et al.*, *Mon. Not. R. Astron. Soc.* **310**, 1147 (1999); P. Bode, J. P. Ostriker, and N. Turok, *Astrophys. J.* **556**, 93 (2001); V. Avila-Reese *et al.*, *Astrophys. J.* **559**, 516 (2001).
- [18] S. Dodelson and L. M. Widrow, *Phys. Rev. Lett.* **72**, 17 (1994).
- [19] X. Shi and G. M. Fuller, *Phys. Rev. Lett.* **82**, 2832 (1999); K. Abazajian, G. M. Fuller, and M. Patel, *Phys. Rev. D* **64**, 023501 (2001); K. Abazajian and G. M. Fuller, *Phys. Rev. D* **66**, 023526 (2002); G. M. Fuller *et al.*, *Phys. Rev. D* **68**, 103002 (2003); K. Abazajian, *Phys. Rev. D* **73**, 063506 (2006); M. Shaposhnikov and I. Tkachev, *Phys. Lett. B* **639**, 414 (2006).
- [20] A. Kusenko, *AIP Conf. Proc.* **917**, 58 (2007); arXiv:astro-ph/0608096; T. Asaka, M. Shaposhnikov, and A. Kusenko, *Phys. Lett. B* **638**, 401 (2006); P. L. Biermann and A. Kusenko, *Phys. Rev. Lett.* **96**, 091301 (2006).
- [21] P. B. Pal and L. Wolfenstein, *Phys. Rev. D* **25**, 766 (1982); V. D. Barger, R. J. N. Phillips, and S. Sarkar, *Phys. Lett. B* **352**, 365 (1995).
- [22] A. D. Dolgov and S. H. Hansen, *Astropart. Phys.* **16**, 339 (2002); K. Abazajian and S. M. Koushiappas, *Phys. Rev. D* **74**, 023527 (2006); K. Abazajian, G. M. Fuller, and W. H. Tucker, *Astrophys. J.* **562**, 593 (2001); A. Boyarsky, A. Neronov, O. Ruchayskiy, and M. Shaposhnikov, *Mon. Not. R. Astron. Soc.* **370**, 213 (2006); *JETP Lett.* **83**, 133 (2006); *Phys. Rev. D* **74**, 103506 (2006); A. Boyarsky, A. Neronov, O. Ruchayskiy, M. Shaposhnikov, and I. Tkachev, *Phys. Rev. Lett.* **97**, 261302 (2006); A. Boyarsky, J. Nevalainen, and O. Ruchayskiy, *Astron. Astrophys.* **471**, 51 (2007); A. Boyarsky, O. Ruchayskiy, and M. Markevitch, arXiv:astro-ph/0611168; S. Riemeer-Sorensen, K. Pedersen, S. H. Hansen, and H. Dahle, *Phys. Rev. D* **76**, 043524 (2007); S. Riemeer-Sorensen, S. H. Hansen, and K. Pedersen, *Astrophys. J.* **644**, L33 (2006).
- [23] U. Seljak *et al.*, *Phys. Rev. Lett.* **97**, 191303 (2006); M. Viel *et al.*, *Phys. Rev. Lett.* **97**, 071301 (2006); P. McDonald *et al.*, *Astrophys. J. Suppl. Ser.* **163**, 80 (2006).
- [24] M. Viel *et al.*, *Phys. Rev. Lett.* **100**, 041304 (2008).
- [25] H. Yüksel, J. F. Beacom, and C. R. Watson, arXiv:0706.4084.
- [26] L. E. Strigari *et al.*, *Astrophys. J.* **652**, 306 (2006).
- [27] A. Palazzo *et al.*, *Phys. Rev. D* **76**, 103511 (2007).
- [28] A. Boyarski *et al.*, arXiv:0709.2301.
- [29] J. R. Bond, G. Efstathiou, and J. Silk, *Phys. Rev. Lett.* **45**, 1980 (1980).
- [30] S. Tremaine and J. E. Gunn, *Phys. Rev. Lett.* **42**, 407 (1979).
- [31] B. W. Lee and S. Weinberg, *Phys. Rev. Lett.* **39**, 165 (1977); P. Hut, *Phys. Lett.* **69B**, 85 (1977); K. Sato and H. Kobayashi, *Prog. Theor. Phys.* **58**, 1775 (1977); M. I. Vysotsky, A. D. Dolgov, and Ya. B. Zeldovich, *JETP Lett.* **26**, 188 (1977).
- [32] E. W. Kolb and M. S. Turner, *The Early Universe* (Addison-Wesley, Reading, MA, 1990).
- [33] A. M. Green, S. Hofmann, and D. J. Schwarz, *J. Cosmol. Astropart. Phys.* 08 (2005) 003; S. Hofmann, D. Schwarz, and H. Stocker, *Phys. Rev. D* **64**, 083507 (2001); A. M. Green, S. Hofmann, and D. J. Schwarz, *Mon. Not. R. Astron. Soc.* **353**, L23 (2004), and references therein.
- [34] G. B. Larsen and J. Madsen, *Phys. Rev. D* **52**, 4282 (1995).
- [35] J. Madsen, *Phys. Rev. Lett.* **69**, 571 (1992).
- [36] J. Madsen, *Phys. Rev. D* **44**, 999 (1991); **64**, 027301 (2001); *Phys. Rev. Lett.* **64**, 2744 (1990).
- [37] P. Salucci and A. Sinibaldi, *Astron. Astrophys.* **323**, 1 (1997).
- [38] C. J. Hogan and J. J. Dalcanton, *Phys. Rev. D* **62**, 063511 (2000).
- [39] J. Lesgourges and S. Pastor, *Phys. Rep.* **429**, 307 (2006).
- [40] S. Hannestad, *Annu. Rev. Nucl. Part. Sci.* **56**, 137 (2006).
- [41] S. Hannestad and G. Raffelt, *J. Cosmol. Astropart. Phys.* 04 (2004) 008; S. Hannestad, A. Mirizzi, and G. Raffelt, *J. Cosmol. Astropart. Phys.* 07 (2005) 002; S. Hannestad *et al.*, *J. Cosmol. Astropart. Phys.* 08 (2007) 015.
- [42] A. Melchiorri, O. Mena, and A. Slosar, *Phys. Rev. D* **76**, 041303 (2007).
- [43] D. Lynden-Bell, *Mon. Not. R. Astron. Soc.* **136**, 101 (1967); S. Tremaine, M. Henon, and D. Lynden-Bell, *Mon. Not. R. Astron. Soc.* **219**, 285 (1986).
- [44] S. Peirani *et al.*, *Mon. Not. R. Astron. Soc.* **367**, 1011 (2006); S. Peirani and J. A. de Freitas Pacheco, arXiv:astro-ph/0701292; E. Romano-Diaz *et al.*, *Astrophys. J.* **637**, L93 (2006); E. Romano-Diaz *et al.*, *Astrophys. J.* **657**, 56 (2007); Y. Hoffman *et al.*, arXiv:0706.0006.
- [45] D. Boyanovsky, M. D'Attanasio, H. J. de Vega, R. Holman, and D.-S. Lee, *Phys. Rev. D* **52**, 6805 (1995).
- [46] D. Boyanovsky, C. Destri, and H. J. de Vega, *Phys. Rev. D* **69**, 045003 (2004); C. Destri and H. J. de Vega, *Phys. Rev. D* **73**, 025014 (2006).
- [47] J. Bernstein, *Kinetic Theory in the Expanding Universe* (Cambridge University Press, New York, 1988).
- [48] S. Dodelson, *Modern Cosmology* (Academic Press, London, 2003).
- [49] W.-M. Yao *et al.*, *J. Phys. G* **33**, 1 (2006).
- [50] R. Cowsick and J. McClelland, *Phys. Rev. Lett.* **29**, 669 (1972).
- [51] D. Boyanovsky, *Phys. Rev. D* **77**, 023528 (2008).
- [52] D. Spergel *et al.* (WMAP Collaboration), *Astrophys. J. Suppl. Ser.* **170**, 377 (2007).
- [53] S. Hansen *et al.*, *Phys. Rev. D* **65**, 023511 (2001); J. P. Kneller *et al.*, *Phys. Rev. D* **64**, 123506 (2001).
- [54] F. de Bernardis *et al.*, arXiv:0707.4170; G. Mangano *et al.*, *J. Cosmol. Astropart. Phys.* 03 (2007) 006.
- [55] J. Binney and S. Tremaine, *Galactic Dynamics* (Princeton University Press, Princeton, NJ, 1987).
- [56] H. J. de Vega and N. Sánchez, *Nucl. Phys.* **B625**, 409 (2002); C. Destri and H. J. de Vega, *Nucl. Phys.* **B763**, 309 (2007).
- [57] D. N. C. Lin and S. M. Faber, *Astrophys. J.* **266**, L21 (1983); J. Madsen and R. I. Epstein, *Astrophys. J.* **282**, 11 (1984).
- [58] S. Hannestad, *New Astron. Rev.* **4**, 207 (1999).
- [59] G. Mangano *et al.*, *Nucl. Phys.* **B729**, 221 (2005).
- [60] K. Ichikawa, M. Kawasaki, and F. Takahashi, *Phys. Rev. D* **72**, 043522 (2005).
- [61] D. Boyanovsky and C.-M. Ho, *Phys. Rev. D* **75**, 085004 (2007); *J. High Energy Phys.* 07 (2007) 030; *Phys. Rev. D* **76**, 085011 (2007); D. Boyanovsky, *Phys. Rev. D* **76**, 103514 (2007).